2024 Jan 08 | 3001

Chapt. 3 Cosmic Present Galaxies as a Benchmark for ~~G~~ Galaxy Evolution & Formation

- Corresponds to Cimatti (2020) p. 28 – 53

Cimatti's chapters are largely high-level description which are best learnt by close reading or equivalent reviews (have to find for yoursel[f])

So in my lectures based on the chapters, I will just expand on certain points where a bit more detail particularly mathematical seems needed and strikes me as interesting. Often ~~the~~ detail will involve mathematical derivation, but not very hard ones.

Also recur[...] figure[...] to co[...] the descri[...] as nee[...] see if thi[...] works

3002

Contents of the 3000 series notes.

1) Specific Intensity + Surface Brightness (3003)
2) Different representations of Specific intensity surface brightness (3008)
3) Surface Brightness, Flux, SED ~~Profiles~~ of Galaxies (30[illegible])
4) and Sersic surface Brightness Profile (302[illegible])
5) Plot of M_r vs M_V for some types of galaxies (3034)
central brightness · overall
6) Plot of Fig 3.5 (C-33) (3036a)
7) Plot of Fig 3.6 (C-34-35) (3036b)
8) Schechter | Luminosity function (3044)
versus
9) Schechter | Mass function (3050)
versus

3003

1) Specific Intensity & Surface Brightness

These are ~~essentially the~~ same thing in different manifestations.

This is explicated Cimatt — 503-505

Consider ~~the~~ frequency representation

specific intensity & surface brightness

$$I_\nu = \frac{dE}{d\nu\, dt\, \underbrace{dA\cos\theta}\, d\Omega}$$

So energy flow per frequency per time per perpendicular area per solid angle.

solid angle

Cone sv ngle directly

dA perpendicular to beam path

θ is the radial angle

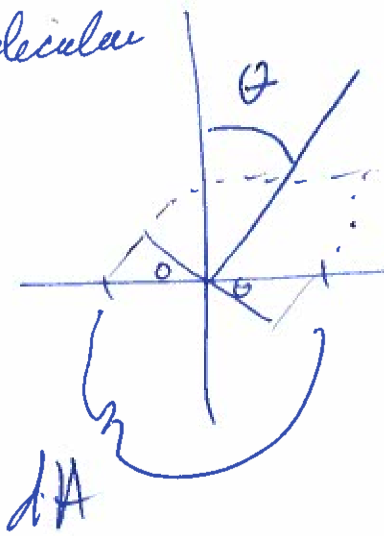

$dA_\perp = dA\cos\theta$ $dA\mu$ where $\mu = \cos\theta$

μ is the radial cosine

surface of em

I call them "radial" because I think of them as measured from the radial ~~direct~~ outward direction of an atmosphere

But HM-342 — 343 calls them polar angle & polar cosine

photon

so in effect classical & quantum probabilities give same answer

on average sphere

travelled in ... fr...

which makes quantum hard to detect without delicate experiments to detect entanglement

HM-60 ff

This macroscopic description where interference, diffraction negligible (random matter ... destr...) polarization not treated, QM effects isolated

opa...

3004

Differential Emitter

specific intensity

Differential Receiver

surface brightness

for a pulse of radiation

~~Point source~~

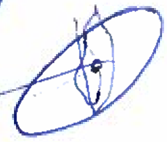

I_ν

No relative motion so Doppler effect of cosmological redshift

No extinction

Invoke energy conservation

$$dE_{em} = dE_{Re}$$

$$\underbrace{I_\nu\, d\nu\, dt\, dA_\perp\, d\Omega}_{emitter} = \underbrace{I_\nu\, d\nu\, dt\, dA_\perp\, d\Omega}_{receiver}$$

$d\Omega = \frac{dA_{\perp Re}}{r^2}$, $\frac{dA_{\perp em}}{r^2}$

Must have

$$\underbrace{d\nu\, dt}_{em} = \underbrace{d\nu\, dt}_{re}$$

$$\underbrace{dA_\perp\, d\Omega}_{em} = \underbrace{dA_\perp\, \Omega}_{re}$$

∴ $I_{\nu\,emitter} = I_{\nu\,receiver}$

specific intensity = surface brightness

and I_ν is distance independent.

Proof that I_ν is constant for { no relative motion of any kind (Doppler, Co…) ; no extinction ; no time dilation of any kind } 3005

Which proves specific intensity (constant) equals surface brightness at receiver

differential emitter

r

differential receiver

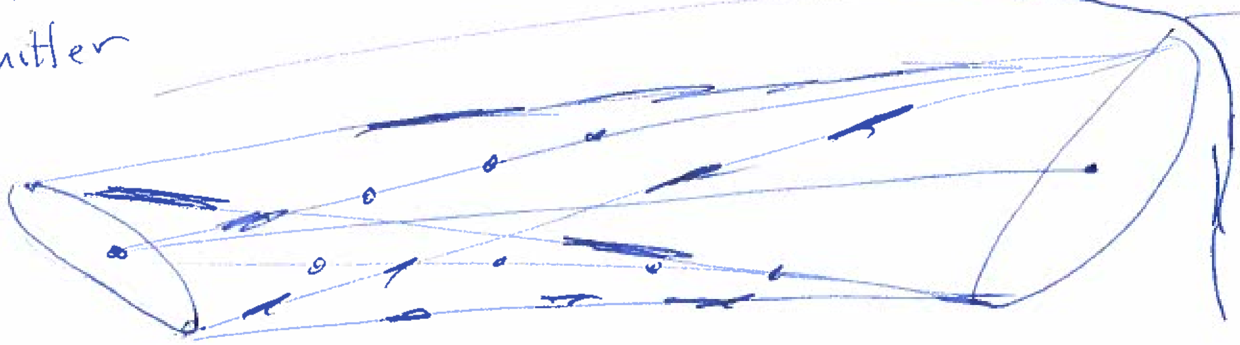

These can be handled when needed

$$\underset{\text{Invoke conservation of energy}}{} \quad \underbrace{dE}_{\text{Pulse of energy emitted by all solid angle cones fud}} = \underbrace{dE}_{\text{Pulse of energy received from all cones}}$$

constant over $A_\perp^{rec}$ for same reasons

$$\underbrace{I_\nu^{em}}_{\substack{I_\nu^{em} \text{ constant over } dA_\perp^{em} \\ \text{and for small changes in angle} \\ \text{since differentially small emitter}}} \underbrace{d\nu\, dt\, dA_\perp}_{em} \underbrace{d\Omega}_{= \frac{dA_\perp^{re}}{r^2}} = I_\nu^{re} \underbrace{d\nu\, dt\, dA_\perp}_{receive} \underbrace{d\Omega}_{\frac{dA_\perp^{em}}{r^2}}$$

no extinction

no frequency shift (Doppler or cosmological or gravitational or other)

$$d\nu_{em} = d\nu_{re}$$

$\therefore$ and $dt_{em} = dt_{re}$ (no time dilation of any kind due to some cause)

$$dA^{em} \frac{dA_\perp^{re}}{r^2} = dA_\perp^{re} \frac{dA_\perp^{em}}{r^2}$$

$$\therefore \quad I_\nu^{em} = I_\nu^{re} \qquad \text{QED}$$

3006).

Of course I_ν can change with extinction, relativistic motion, time dilation, but those are effects ~~that~~ are treated as needed.

~~- of course if you have redshift/blueshift and extinction there are complications~~

Special Case of Interest

Connecting I_ν to L_ν & $\mathcal{F}_\nu$

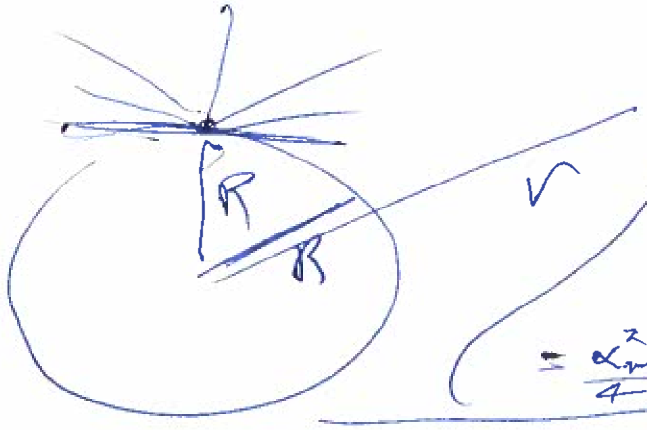

Distant observer

Angular diameter: $\alpha_\nu = \left(\frac{2R}{r}\right)$, $\left(\frac{R}{r}\right)^2 = \frac{1}{4}\alpha^2$

d) $\hat{\mathcal{F}}_{\nu\,\text{obser}}$

$$= \frac{L_\nu}{4\pi r^2} = \pi I_\nu \left(\frac{R}{r}\right)^2 = \mathcal{F}_\nu \left(\frac{R}{r}\right)^2$$

as you would expect,

$$= \frac{\alpha_\nu^2}{4}\hat{\mathcal{F}}_\nu$$

(M-11-12, HM-74-75)

spherically symmetric source (e.g., a star)

a) surface flux $\hat{\mathcal{F}}_\nu = \oint I \cos\theta \, d\Omega$

No limb darkening: $= 2\pi \int_0^1 I_\nu \mu \, d\mu = 2\pi I_\nu \frac{\mu^2}{2}\Big|_0^1$ For constant I_ν

b) $\int_0^\pi \ldots \cos\theta \sin\theta \, d\theta = \int_{-1}^{1} \ldots \mu \, d\mu$ $\cancel{\int_{-1}^{1} \ldots d\mu}$

$\mu = \cos\theta$, $d\mu = \sin\theta \, d\theta$, $\mu \, d\mu = \cos\theta \sin\theta \, d\theta$

but no inflow from space and so $\int_0^1 \ldots \mu \, d\mu$

c) $\mathcal{F}_\nu = \pi I_\nu$

$$L_\nu = 4\pi R^2 (\pi I_\nu)$$

SED = spectral energy density

Just luminosity per frequency (or wavelength) (Cimatti-35)

or maybe sometimes just total flux per Hz or Å measured by observer (Even Wikipedia is unclear)

9008

2) Different Representations of specific intensity / surface brightness

These differential of integrated "energy" must be the same

$$I_E\, dE = I_\nu\, d\nu = I_\lambda (-d\lambda)$$

photon energy   frequency   wavelength

Relation here easy

$E = h\nu$

$dE = h\, d\nu$

$I_E = \dfrac{I_\nu}{h}$

Note $\lambda = \dfrac{c}{\nu}$

$d\lambda = -\dfrac{c}{\nu^2} d\nu$

$\therefore$ ~~corresponding~~ differentials in $d\lambda$ and $d\nu$ have different signs.

If $d\nu > 0$

$d\lambda < 0$

$\therefore -d\lambda > 0.$

$$I_\nu = I_\lambda \frac{c}{\nu^2} = I_\lambda \frac{\lambda^2}{c}$$

Hybrid or logarithmic representation

$$(E I_E)\underbrace{\frac{dE}{E}}_{d\ln E} = \nu I_\nu \underbrace{\frac{d\nu}{\nu}}_{d\ln\nu} = \lambda I_\lambda \underbrace{\left(-\frac{d\lambda}{\lambda}\right)}_{-d\ln\lambda}$$

Mostly for plotting purposes

But note

$E = h\nu = h\frac{c}{\lambda}$ 3009

$\ln E = \ln h + \ln \nu = \ln(hc) - \ln\lambda$

$d\ln E = d\ln\nu = -d\ln\lambda$

$\therefore \quad E I_E = \nu I_\nu = \lambda I_\lambda$

So all equal.

The logarithmic representation is often used in ~~plots~~ it seems.

Three reasons?

a) some value ~~for~~ E, ν, λ independent variable.

b) ~~and~~ In some cases it flattens the profile

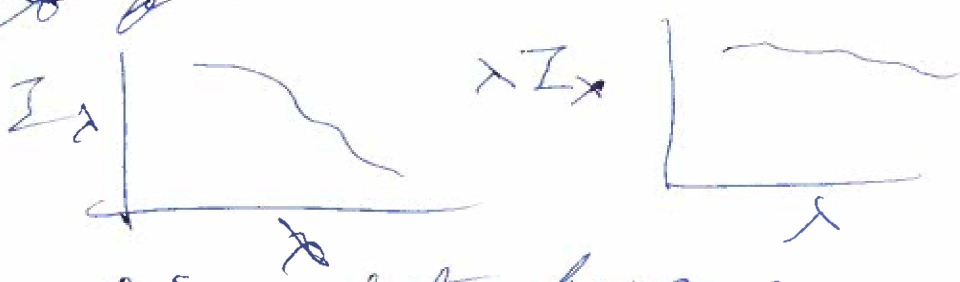

making plots have a smaller vertical range.

c) Integration by eye with logarithmic scale is sometimes easy.

$dE = (\nu I_\nu)_{ave} \Delta\ln$ energy in this band

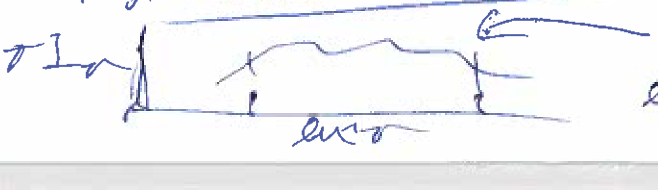

30 8)

3) Surface Brightness Profiles of Galaxies (SBP)

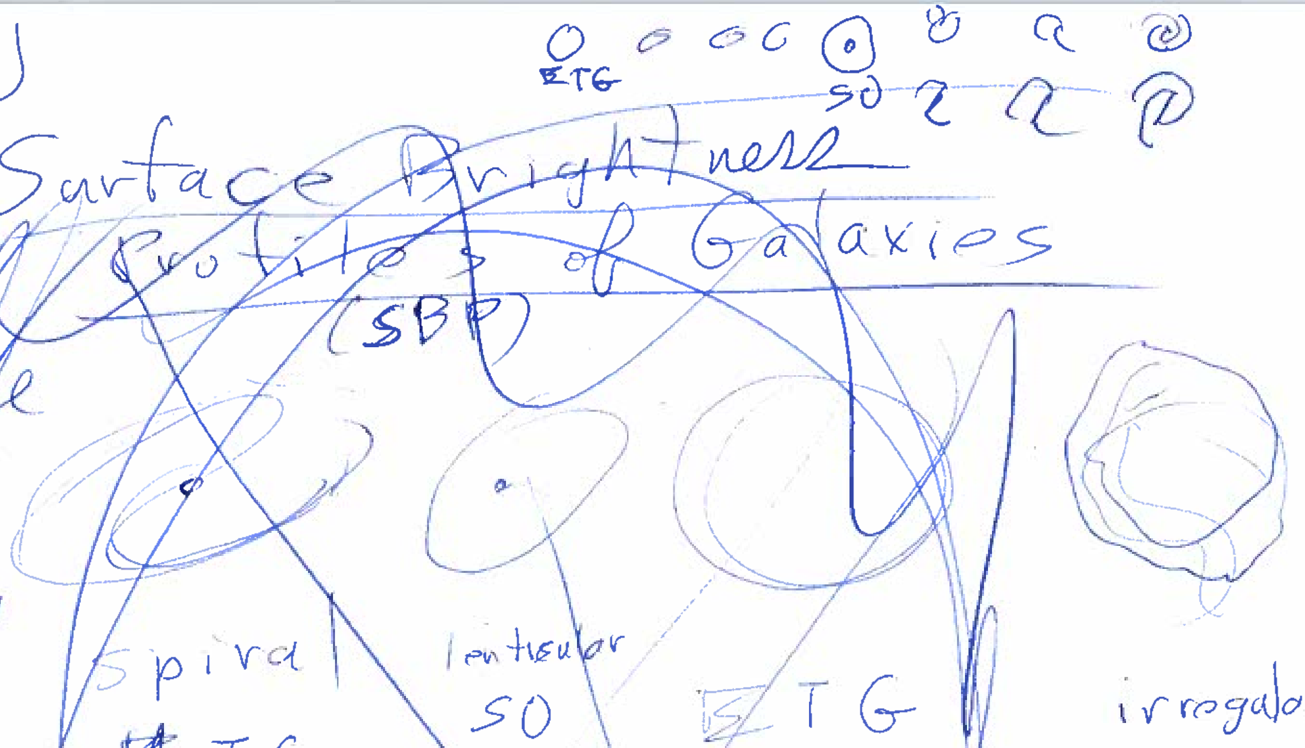

In general we don't know the orientation without some deductions

a) Surface Brightness Profile

Recall we see galaxies in projection on the sky (the celestial sphere) and so their surface ~~density~~ brightness profiles ~~and~~ are a "convolution" of intrinsic emission and projection effects.

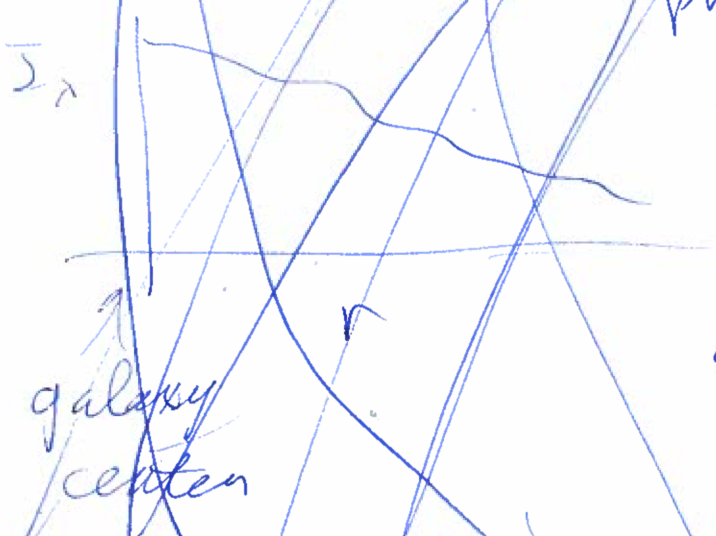

And they are in general they do not have spherical symmetry on the sky

3011

3) Surface Brightness ~~Profiles~~ Flux, Spectral Energy distribution of Galaxies

smaller Bulge
less tightly wound (Sb

a) Hubble sequence plus de Vaucouleur

Challenge
To class
sketch from memory

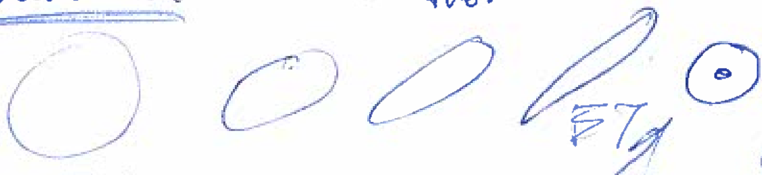

E0 E7

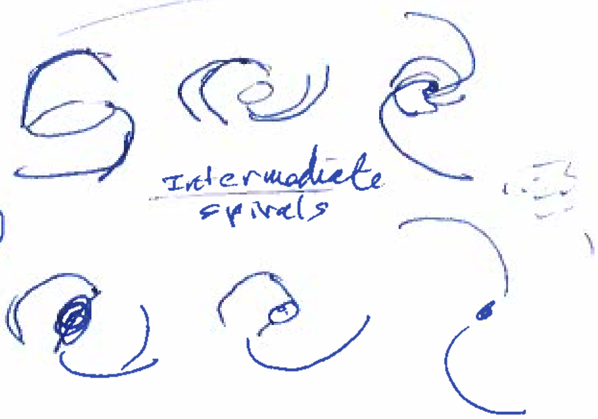

Intermediate spirals

Lenticular or S0

Barred spirals

Irregular

~~Early Type~~

Jillions of special galaxy type and galaxies often fall into multiple type categories

Early type (ETGs)

smaller than spirals
~~[illegible]~~
1 hot star formation similar
– blues, pink brown regions enhanced true color

Can be like 1-arm spiral

Hubble Jargon with no theoretical implication

so early doesn't mean formed first

Late type (LTGs or SFGs) star forming galaxies

late doesn't mean formed later.

In fact, it is more the other way around. Ellipticals form often by merging spirals and ellipticals are mostly nearly quenched galaxies – star formation turned off.

3012)

~~the orientation~~

the shape of spirals in 3d can usually be known since we can recognize their type in any orientation

but with ellipticals and irregulars ~~their~~ 3-d shapes ~~are~~ not well constrained by their projection on the sky

b) Surface Brightness Profile (SBP) Itself

is just ~~SB~~ surface brightness as a fraction of radius r out from the center

The projected image is not round in general

R

usually circularized radius ~~(see p. 3013)~~ or elliptical radius see p. 3013–3015

the galaxy or object projected on the sky

— So intrinsic and orientation ~~SB~~ emission effects are convolved

Alg

galaxies are optically thin in stars but ~~necessarily~~ in gas + dust

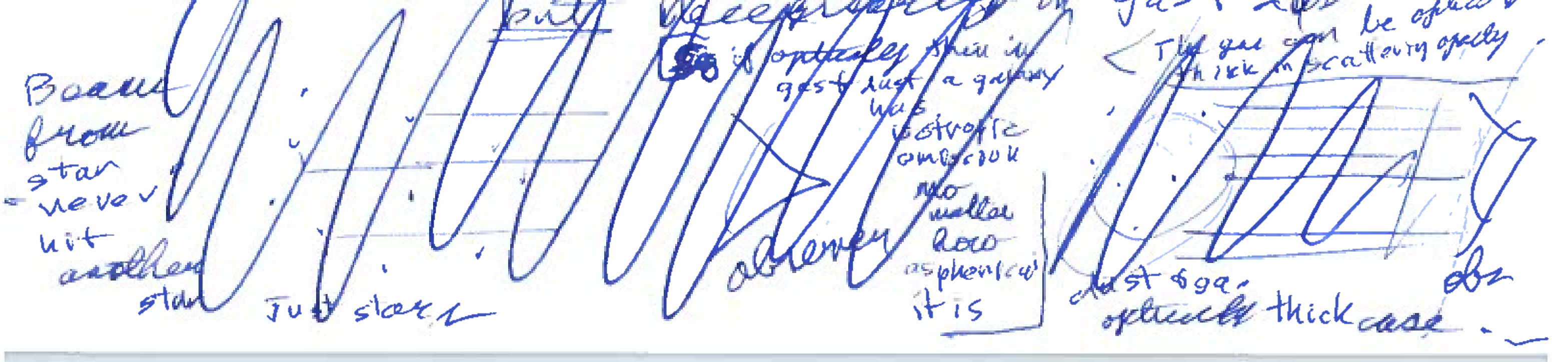

Nevertheless, the SBP ~~spherical surface~~ s ~~various~~ $\cancel{X}$ (or V) bins and direction in is important characterizing information and with appropriate reduction/modeling lead the intrinsic information. (Though how I don't know) we're all on a learning curve

Large scale structure models (Illustris, TNG, Eagle) can be used create synthetic SBP where statistical properties can be compared to observation

Isophotes = contours ~~of~~ of constant SB (surface brightness

iso constant

light

Not eccentricity $e = \frac{\sqrt{a^2-b^2}}{a} = \sqrt{1-b^2/a^2}$ (Wiki ellipse)

ellipticity of an isophote (C-31)

$$\varepsilon = \frac{a-b}{a} = 1 - \frac{b}{a}$$

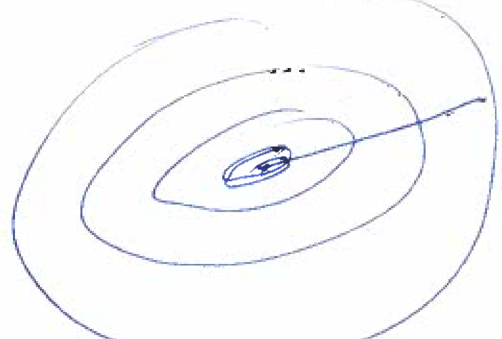

a is semimajor axis

b is semiminor axis

if isophotes (call for a galaxy) ~~approximate~~ ~~a~~ ellipses which seems often a good approximation or fit.

$b = a(1-\varepsilon)$

elliptical radius $a \equiv R_a$

R_c circularized radius $(ab)^{1/2}$

Area of ellipse $= \pi a b = \pi R_c^2$

~~See Wiki ellipse's area~~

$dA_{\text{elliptical}} = 2\pi R_c \, dR_c$

Either R_a or R_c can be used to label isophotes and construct a profile. C-31. I'm usually going to think of circ

301(14)

d) Effective Radius R_e

(or half-light radius)

I'm going to think of it as a circularized radius R_{circ}

but R_{ae} ← elliptical radius to

R_c = $R_{circularized}$ R_e

C-31 says both definitions are used and in rough analyses the distinction may be negligible, i.e. $R_{ce} \neq R_{ae}$

Exactly the same for circularly symmetric galaxy projection

$$F_{\lambda,\text{observer}} = \int I_\lambda \, d\Omega$$

dR

galaxy

earth

but $d\Omega = \frac{dA_\perp}{r^2} = \frac{2\pi R\,dR}{r^2}$

$\frac{dE}{d\lambda\,dt\,dA_\perp}$

observer device which can be integrated over

↳ in fact the device integrates and you have to divide by its $A_\perp$ device to F_λ

where R is probably usually the circularized radius R_{ce} ~~or~~ the elliptical R_{ae} ~~elliptic approximation~~

$R = (ab)^{1/2}$

$A = 2\pi R\,dR$ $A = \pi a b$

Sep. 30

Two kinds of Radius; Either one can be used

Elliptical Radius (coordinate) | Circularized radius

$R_a = a$

$R_c \equiv (ab)^{1/2}$

$$\text{Area} = \pi a b = \pi a[a(1-\varepsilon)] = \pi R_a^2 (1-\varepsilon)$$

$$dA = 2\pi R_a (1-\varepsilon)\, dR_a$$

Area of an ellipse

$A = \pi a b = \pi R_c^2$ (Wiki: Ellipse area)

$$dA = 2\pi R_c\, dR_c$$

Cimatti-31 says either can be use to label isophotes ~~and for R_e effective radius or half light radius (see p.~~

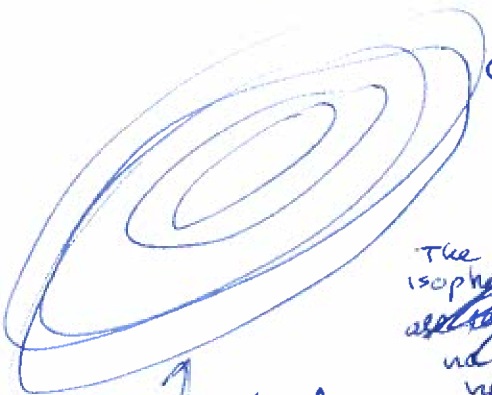

The isophotes are ~~all the same~~ no matter how labeled ~~Same isophotes and the R_e labeled isophote contains half the luminosity and same profile and R_a & R_c in general unless the galaxy projection is circularly symmetric on the sky.~~

Note, the isophotes are the same no matter labeled ~~Likewise~~ the effective radius (or half-light radius; see p. 3020) and SB profile but the label values are different if the projection is not circularly symmetric

I will ~~think~~ in terms of circularized radius hereafter to be definite.

3016

1) Flux and Spectral Energy Distribution (SED)

$$F_\lambda(R) = \int_0^R J_\lambda \left(\frac{2\pi R\, dR}{r^2}\right)$$

circularized radius – No $(1-\varepsilon)$ factor (see p. 3015)

$$\frac{dE}{d\nu\, dt\, dA\, \cancel{d\,\text{source}}}$$

← collecting device

surface brightness $J_\lambda = \frac{dE}{d\nu\, dt\, dA\, d\Omega}$

area of device

subtended from the observer

differential solid angle subtended at observer

observer

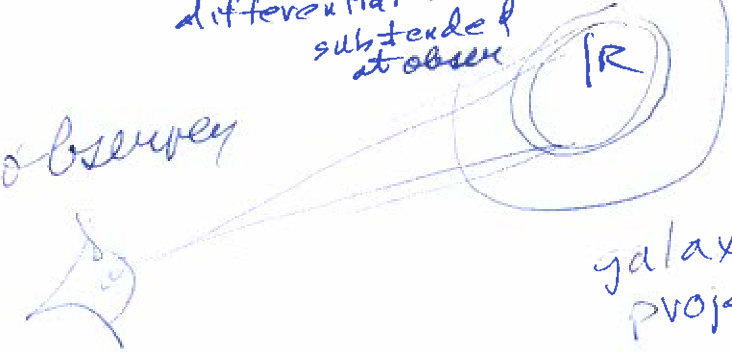

galaxy projection

Actually the device measures $\mathcal{F}_\lambda = F_\lambda(R)\, A_{device}$

~~and~~ one uses to get flux $F_\lambda = \mathcal{F}_\lambda / A_{device\,(observer)}$

$\mathcal{F}_\lambda$ is device dependent, so you want F_λ

F_λ

flux measured by observer

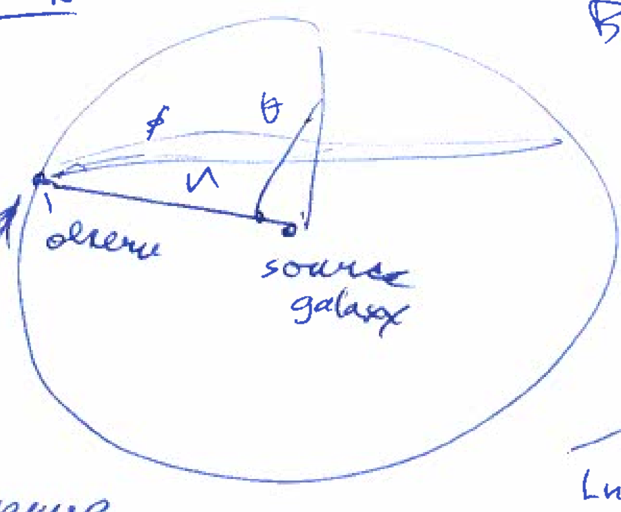

observer

But say you had a device all around the galaxy at radius r

$$L_\lambda = \oint F_\lambda(\theta\phi)\, dA_{obs\ sphere}$$

Luminosity per wavelength

and this seems to

be one definition for

SED = spectral energy density
(e.g., C-35 for example)

but sometimes

F_λ is called SED

{Wik is unclear!, but seems ~~to the latter~~ }

When is a galaxy isotropic in emission?

Galaxies are always optically thin in stars,
A beam from a star almost never hits another star, no matter how dense stars are

~~What if there is just scattering opacity~~

so a just-stars galaxy emits isotropically no matter how aspherical it is.

Stars themselves emit isotropically to very high accuracy

What if just scattering opacity (usually from electrons.
That just randomizes the scattered light, and so the emission is again isotropic.

ele[illegible] is No iso[illegible]

Elliptical galaxies tend to be like this,
They have little dust and their gas is mostly ionized hydrogen and almost invisible except in X-rays

3U(8) LTGs (SFGs) with gas & dust are opaque in absorption opacity, and so will usually be anisotropic emitters

Stars, of course, are ~~almost~~ ~~exac~~ isotropic emitters to high accuracy.

~~be one definition of SED~~ ~~(p. 3019)~~ ~~(G-35)~~ ~~see away~~

~~but sometimes it seems F_λ is called SED.~~

~~W.M. SED is a bit unclear but seems to mean the latter.~~

If the source is spherically symmetric (true to high accuracy for stars
— true for optically thin galaxies (see p. 3017–3018)

then $L_\lambda = F_\lambda (4\pi r^2)$

but if ~~s~~ource is not isotropic

then $L_\lambda^{\text{equivalent}} = F_\lambda (4\pi r^2)$

the isotropic equivalent luminosity which gets a lot of use for GRBs ~~with~~ which are not at all ~~isotropic~~ source
— strongly beamed in the jet direction

in absorption opacity

~~Optically galaxies~~ may approximate this also

They have little dust, gas transparent in optical ~~in absorption~~ ~~but~~ highly ionized (H & He)

electron scattering opacity may be high. but that just randomizes direction ~~of photons~~

4) Surface Brightness Profiles (SBPs) (No C-498 acronym)
of the Sersic Profile

$R_e = R_{\text{effective}}$ is such that
$F_\lambda(R_e) = ~~F_\lambda(...)~~$
$= \frac{1}{2} F_\lambda(R \to \infty)$

R
(either circular or elliptical as the ~~author~~ prefers (see p. 3015))
(But I think in terms of circularized radii)

The Sersic profile was introduced by Sersic, 1968, Atlas de galaxias Australes, Obs. Astr. Cordoba (probably in spanish)
as a generalization of the de Vaucouleurs profile (1948 in French)

It turns out to be a very good fitting function for SBPs in general for ~~reason~~ that can be justified theoretically a little bit. Probably in special cases, it can be theoretically justified to a better degree, but we won't go into that.

$$F_\lambda = \int_0^R f_\lambda \frac{2\pi R\,dR}{r^2}$$

Say you integrated

$L_\lambda = \int F_\lambda \, A_{sphere}$ of radius r

luminosity per λ which is what sometimes people mean by SED = spectral energy distribution but sometimes ~~they~~ just mean $F_\lambda A_{detector}$ I ~~think~~

(Wiki: SED manages to be unclear and Cox-37-37 is no help either)

If the source is actually isotropic or spherically symmetric $F_\lambda(r)$ is constant

$L_\lambda = F_\lambda 4\pi r^2$

Some galaxies approximate being isotropic (E0 ellipticals) but many clearly are not,

Still one can define $L_\lambda^{\text{isotropic equivalent}} = 4\pi r^2 F_\lambda$

— which one does for gamma-ray bursts which are very non-isotropic sources.

3022

Sersic Profile

~~surface brightness profile~~

~~Introduced in 1968 in Atlas de galaxias Australes Obs. Ast. Cordoba (no probably in Spanish)~~

It is {parameterization / fitting function} of surface brightness profiles in terms of 4 initial parameters that ~~are reduced to two parameters~~ are reduced to 3 then 2:

1st ~~Total~~ brightness in x, but that is set by distance which is any person problem

The three are ~~effective~~ ~~equivalent~~ ~~radius~~ effective radius ~~2 actual~~ usually ~~the~~ ~~circularized~~ one.

R_e, b, and a power n

$$I_x = \underset{\text{at } x=1}{I_{xe}}\, e^{-b(n)(x^{1/n}-1)} \quad (C=31)$$

$$= \underbrace{I_{x0}}_{\text{at } x=0}\, e^{-b(n)x^{1/n}}$$

(form of Ciotti-2 which I will use)

think in terms of circularized radius, but no difference if you use elliptical radius

where $x \equiv \dfrac{R}{R_e}$

Demanding R_e be the effective radius (half-light radius — see below constrains $b = b(n)$)

and then $b = b(n)$ is a function of n and so is not a free parameter.

Possible n values

$n = 0$ which give $I_\lambda = 0$ everywhere except $x = 0$ — maybe uninteresting limit

$n = \frac{1}{2}$ Gaussian

$n = 1$ exponential

$n = 4$ corresponds to de Vaucouleur (1948) profile $I_\lambda = I_{\lambda 0} e^{b x^{1/4}}$

~~$I_\lambda = I_{\lambda 0} (x)^{1/4}$~~

which he found ~~found~~ to be rather valid for all ellipticals with his 1948 data

Fits

discs $n \leq 1$

bars of disc $n \lesssim 0.5$

ellipticals and central bulges $n \in [2, 10]$ very steep

Includes 4 as middle case

Fiducial division/separative value ~~separation~~ between ETG and later types $n_s = 2.5$

$n > n_s$ for ETGs

$n < n_s$ for LTGs

C-32

as $n \uparrow$ – the profile steepen in center
– shallower farther out (C-31 Fig 3.3 which I show concretely on p. 3023a)

$\frac{\partial I}{\partial x} = -b \frac{1}{n} x^{1/n - 1} I$

as $x \to 0$, diverges: ~~less~~ to x^{-1} as n increases

No divergence for $n \leq 1$

3024

Why is ~~the~~ Sersic profile ~~a good~~ fitting function.

Well Ciotti (1999) gives some references for ~~why it should~~ theoretical justifications.

But we can list some general ~~points~~ observations as to why ~~a priori~~ it would be a good guess.

a) $I_\lambda^{obs}(R=0) < \infty$

and $I_{\lambda\,sersic}^{sersic}$ has ~~that~~ property, though it ~~has a cusp~~ ~~at R=0~~ can have a cusp at $R=0$

b) $I_\lambda^{obs}(R)$ falls monotonically outward ~~as observation~~ usually, but does not go to zero in any definite fashion and the exponential gives that.

$$\frac{\partial I_\lambda^{ser}}{\partial R} = I_0\left(-b\frac{1}{n}x^{1/n-1}\right)e^{-bx^{1/n}}$$

< 0 always

$\to 0$ as $x \to \infty$

~~where~~ at $x=0$ $\begin{cases} -\infty \text{ for } n<1 \\ -b \text{ for } n=1 \\ 0 \text{ for } n>1 \end{cases}$ slope

[illegible] $\sim \frac{1}{x}$ for $n \to \infty$

flat $\to 1$

I_λ no cusp.

flat maximum

e can make
. DE
$' = -b\frac{x^{1/n-1}}{n} I$
t I do
not think
i has any
eral
meaning
e I'll show
soon.

Note $\frac{\partial I_x}{\partial x} = -b\frac{x^{n-1}}{n} I_x$ does this DE have any meaning. No, I think, Different ~~effects~~ give different power laws (cusp

3024d

c) Graphical behaviour $n=10$

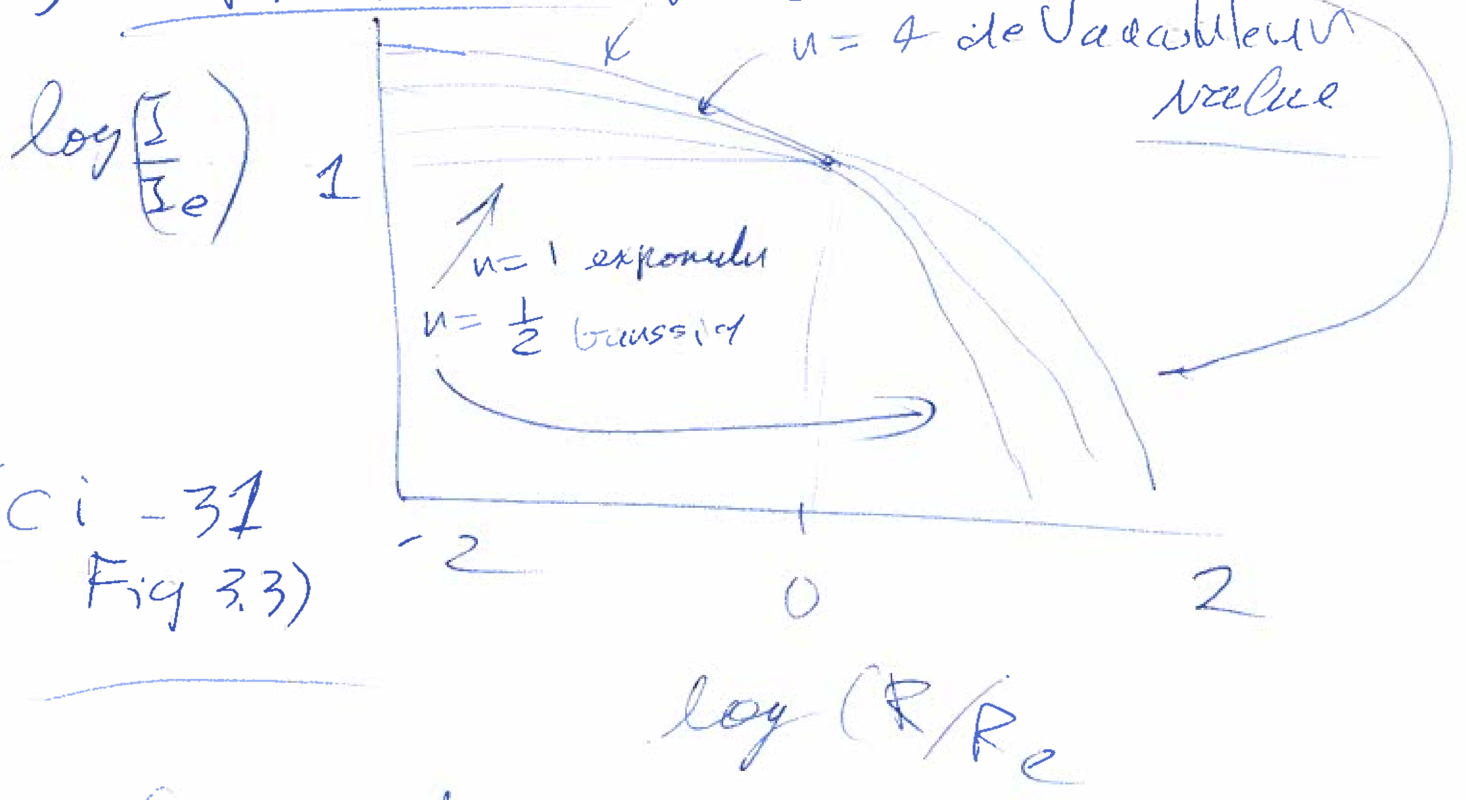

(Ci -31 Fig 3.3)

~~So steepen~~

$n\uparrow$ steepen $x<1$, shallower $x>1$

d) ~~To~~ prove this

$I_x = I_{x_0} e^{-bx^{\frac{1}{n}}} =$

Inner $x<1$

$I_{x_0}(1 - b\,x^{\frac{1}{n}})$ $x \ll 1$

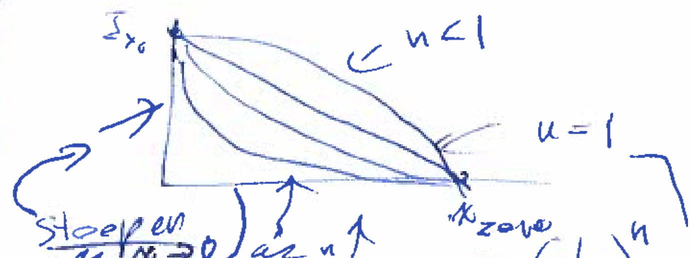

$n=\frac{1}{2}$ gives $\frac{1}{n}=2$ a parabola

$n=1$ a line $\frac{1}{n}=1$

$n=2$

$\frac{1}{n}=\frac{1}{2}$ power

Outer $x>1$

$n\uparrow$, $x^{\frac{1}{n}}\downarrow$, $x \gg 1$

$\therefore \uparrow I e^{-bx^{\frac{1}{n}}}$

shallower

The exponent pushes zero off to $x\to\infty$

Contd on p3

3024b

d) ~~It does~~ have power law ~~behavior for~~ $x \lesssim 1$

$$I_\lambda = I_{\lambda_0}\left(1 - b x^{1/n}\right) \quad \text{for } x \lesssim 1$$

for $x \gg$ $I = I_0 e^{-b x^{1/n}}$

$n\uparrow$, $x^{1/n}\downarrow$ ~~and the~~ decline shallow

$n = \frac{1}{2}$ gives a parabola

$n = 1$ linear

~~We need the exponential to prevent the definite zero.~~

I_{λ_0}

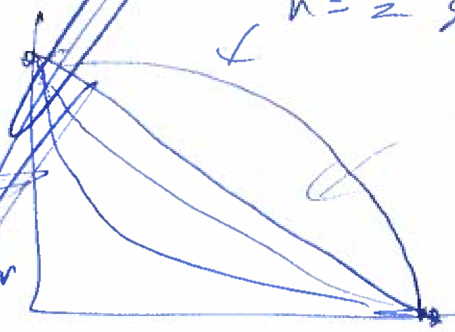

~~steeper~~ gets steeper ~~as~~ as n goes from 1 to ∞.

$$x_{zero} = \left(\frac{1}{b(n)}\right)^n$$

~~recall b = b(n)~~

$$\boxed{0 = 1 - b x^{1/n} \qquad x_{zero} = \left(\frac{1}{b}\right)^n}$$

Cont. from p. 3023d Which is good since ~~Recall~~ as $I(R \to \text{large})$ no definite zero point.

So I suspect the exponential is not so much arising from some exponential effect, but a ~~too~~ smooth way of morphing from the inner power law ~~below~~ ~~the local~~ outer behavior ~~which~~ could be a different power law.

to indefinite ~~decline~~ decline

3026

Why is power law behavior a good idea, but not a specific universal one for all galaxies.

Well, my guess is that there are competing ~~effects~~ power law effects ~~that~~ and ~~that~~ some conditions (e.g., mass, quenching or star forming, formation history, mergers, disk, ellipticals, dust/no dust, history, projection effects) favor one more than the other and ~~it~~ the favored one wins out roughly.

This is why I think the Sersic profile does not follow from a definite differential equation (see p. 30 ~~23~~ 24 top)

= Power law ingredients

i) gravity $\sim 1/r^2$

ii) Projection $A \propto r^2$

iii) Volume $V \propto r^3$

iv) Density profiles

$$\rho_{NFW} = \frac{4\rho_s}{\frac{r}{r_s}\left(1+\frac{r}{r_s}\right)^2}$$

$\propto \frac{4\rho_s}{r/r_s}$ for r ... cusp like (singular)

ρ_s for $r = r_s$

$\frac{4\rho_s}{(r/r_s)^3}$ $r \gg r_s$

$$\rho_{Burkert} = \frac{4\rho_s}{\left(1+\frac{r}{r_s}\right)\left(1+\left(\frac{r}{r_s}\right)^2\right)}$$

$4\rho_s$ $r = 0$

$4\rho_s\left(1-\frac{r}{r_s}\right)$ $r \ll r_s$

core like (but really cusp like)

ρ_s $r = r_s$

$\frac{4\rho_s}{(r/r_s)^3}$ $r \gg r_s$

$$\rho = \rho_s\left(\frac{r}{r_s}\right)^{-2} = \rho_s\left(\frac{r_s}{r}\right)^2$$

$\to$ flat velocity profile

$M(r) = \int_0^r \rho\, 4\pi r^2 dr = \rho_s 4\pi r_s^3\left(\frac{r}{r_s}\right)$

$$M = 4\pi \rho_s r_s^3\left(\frac{r}{r_s}\right) = M_s\frac{r}{r_s}$$

circular orbit velocity law

$$\frac{v^2}{r} = \frac{G M_s (r/r_s)}{r^2}$$

$$v = \sqrt{G M_s / r_s} \quad \text{a constant which is}$$

what is observed for outer disk galaxies and indicates Dark matter which ρ profile that approximates $\rho \propto \frac{1}{r^2}$ somehow

d) Effective radius and the function b(n)

See p. 3016 & 3018

$$\frac{L_x^{iso}(R)}{4\pi} = F_x(R) r^2 = 2\pi\int_0^R I_x R\, dR$$

see p. 3025

~~$\mathcal{L}_x$ for simplicity~~

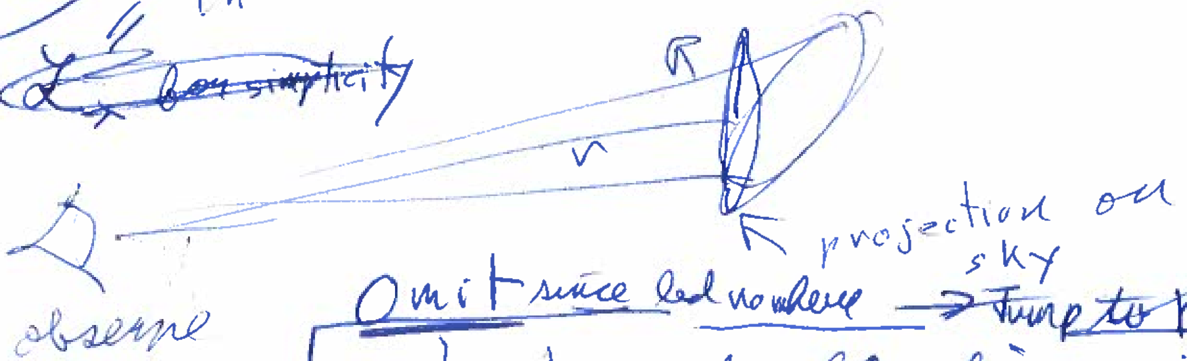

Omit since led nowhere $\to$ Jump to p. 3030

Let's do the linearized approximation first to see how things go.

3028

$$I_\lambda = I_{\lambda_0}\left(1 - b\,x^{\frac{1}{n}}\right)$$ see p. 3035

$$x_{zero} = (1/b)^n$$

$$\mathcal{L}_\lambda = \left(\frac{L_\lambda^{iso}(R)}{4\pi}\right) = 2\pi I_{\lambda_0} R^2 \int_0^{x_{zero}} \left(1 - b\,x^{\frac{1}{n}}\right) x\,dx$$

$$\mathcal{L}_\lambda(x) = \frac{\frac{L_\lambda^{iso}(R)}{4\pi}}{2\pi I_{\lambda_0} R^2} = \int_0^{x} \left(1 - b\,x^{\frac{1}{n}}\right) x\,dx$$

$$\mathcal{L}_\lambda(x) = \int_0^{x} \left(1 - b\,x^{\frac{1}{n}}\right) x\,dx$$

$$\mathcal{L}_\lambda(x) = \left[\frac{x^2}{2} - b\,\frac{x^{\frac{1}{n}+2}}{\frac{1}{n}+2}\right] = \frac{x^2}{2}\left[1 - \frac{b\,x^{\frac{1}{n}}}{1+\frac{1}{2n}}\right]$$

$$\mathcal{L}_\lambda(x_z) = \left[\frac{(1/b)^{2n}}{2} - b\,\frac{\left(\frac{1}{b}\right)\left(\frac{1}{b}\right)^{2n}}{\frac{1}{n}+2}\right]$$

$$= \frac{\left(\frac{1}{b}\right)^{2n}}{2}\left[1 - \frac{2}{2+\frac{1}{n}}\right] > 0$$

except for $n = 0$

$\boxed{3029}$

$$\mathcal{L}_x(x_2) = \frac{(1/b)^{2/n}}{2}\left[1 - \frac{1}{1+\frac{1}{2n}}\right] > 0$$ which is good

$$\mathcal{L}(x_e = 1) = \cancel{\frac{1}{b}\mathcal{L}(x_e)} = \left[\frac{1}{2} - \frac{b}{n+2}\right]$$

demand this to constrain b

$$= \frac{1}{2}\left[1 - \frac{b}{1+\frac{1}{2n}}\right]$$

and $\mathcal{L}(x_e=1) = \frac{1}{2}\mathcal{L}(x_2)$

$$\frac{1}{2}\,\frac{(1/b)^{2/n}}{2}\left[1 - \frac{1}{1+\frac{1}{2n}}\right] = \frac{1}{2}\left[1 - \frac{b}{1+\frac{1}{2n}}\right]$$

~~and b = 1 independent~~

If $x_{zero} > x = 1$

$x_{zero} = \left(\frac{1}{b}\right)^n$

This linearized ~~attempt~~ is ~~no good~~

Lead nowhere.

3030

~~To get insight, let's first try the easiest case n=1~~

Reduced → for simplicity

$$\mathcal{L} \equiv \frac{\left(\frac{L_\lambda^{iso}(R)}{4\pi}\right)}{2\pi I_{\lambda 0} R_e^2} = \int_0^x e^{-b x^{\frac{1}{n}}} x\, dx$$

where $x \equiv \frac{R}{R_e}$

To eliminate b as a free parameter and get $b = b(n)$, we demand

$$\underbrace{\tfrac{1}{2}\mathcal{L}(x=\infty)}_{\text{total light}} = \mathcal{L}(x=1)$$

half-light

effective radius in units of R_e

General n is tough, let's try the easiest case $n=1$ to see how it is done.

$$\mathcal{L} = \int_0^x e^{-bx} x\, dx$$

$$= -\frac{e^{-bx}}{b} x \Big|_0^x + \int_0^x \frac{1}{b^2} e^{-bx} dx$$

{integration by parts (Wiki)}

$$= -\frac{e^{-bx}}{b} x + \frac{1}{b^2}\left(1 - e^{-bx}\right)$$

$$= \frac{1}{b^2} - \frac{1}{b^2}(bx+1)e^{-bx}$$

3031

$$\therefore \frac{1}{2}\mathcal{L}(x=\infty) = \frac{1}{2}\frac{1}{b^2} = \mathcal{L}(x=1) = \frac{1}{b^2} - \frac{1}{b^2}(b+1)e^{-b}$$

shifting to origin means you already know where it is OK in a proof

$$\frac{1}{2} = 1 - (b+1)e^{-b}$$

$$\frac{1}{2} = (b+1)e^{-b}$$ which is a transcendental equation and has ~~no~~ no analytic solution

Integrate function converges

Let's rewrite it as a convergent iteration formula for variable b

Convergence

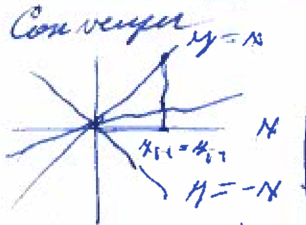

$$e^b = 2(b+1)$$

$$b = \ln[2(1+b)]$$

$$b = \ln 2 + \ln(1+b)$$

$|y_i| = |f(y_{i-1})| \le |y_{i-1}|$ then (convergence / divergence)

if $\frac{\partial t}{\partial x} < 0$, oscillating sign

necessary and sufficient for monotonic convergence $\left|\frac{\Delta t}{\Delta x}\right| < 1$

$\left|\frac{d\,b_{out}}{d\,b_{in}}\right| = \left|\frac{1}{1+b}\right| < 1$ for $b > 0$

~~Graphical~~ Newton-Raphson faster

then sufficient for convergence

Sort of true for multivariable iteration too as in solving atmosphere by lambda iteration

We reasonably assume this is the convergent form since the RHS varies slowly with

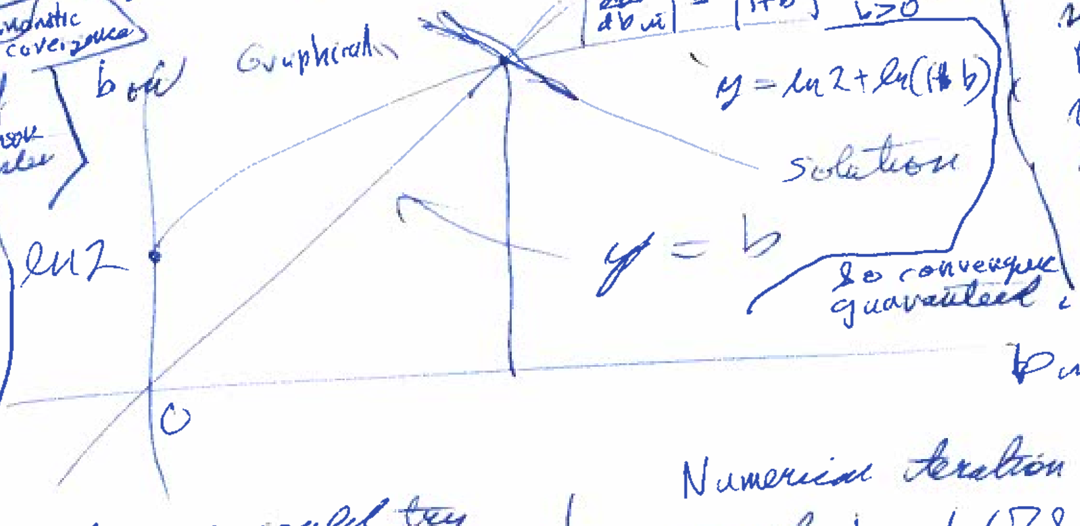

Numerical iteration $b_0 = \ln 2$ and $b_{30} = 1.678\,346\,990$.

seems ~~or~~ converged to these values.

in adiabatic transfer with Monte Carlo which conserves energy

If $b < 1$, we could try a series expansion

but graphically it doesn't look as if $b < 1$

Ciotti eq (8)

worse

$b_{cit} = 1.678\,346\,0$

$b_{eq\,5} = 1.678\,460\,1$

$$b = \ln 2 + \frac{b^2}{2}$$

(Wiki: log) (Wiki: log 2)

$$b = \sqrt{2\ln 2}$$

$= \sqrt{2 \cdot 0.6931\ldots} \cong 1.2 > 1$, and so inconsistent with expansion

3032

What about general n
Ciotti & Bertin 1999 have tackled this

$$\mathcal{L} = \int_0^{x} e^{-b x^{1/n}} \, x \, dx$$

$$\text{let } z = b x^{1/n}$$

$$\therefore \; x = \left(\frac{z}{b}\right)^n$$

$$dx = n \left(\frac{z}{b}\right)^{n-1} \frac{dz}{b}$$

$$\mathcal{L} = \frac{n}{b^{2n}} \underbrace{\int_0^{z} e^{-z} z^{2n-1} \, dz}_{\text{Incomplete gamma function}} = \frac{n}{b^{2n}} \int_0^{z} e^{-z + (2n-1)\ln z} \, dz$$

$$\gamma(2n, z)$$

$$\Gamma(2n) = \gamma(2n, z = \infty)$$

$$= (2n-1)!$$

The generalized Factorial function

Undefined only for negative integers [-1, -2, ...]
See Arf ~~-~~ 943

Arf - 539
- 540
- 943

[30 33

So ~~the~~ solution for

$$\frac{1}{2}\Gamma(2n) = \gamma(2n, z=b)$$

(Ciotti equ

is $b = b(n)$ for which there is no analytic solution

but $\frac{1}{2}\Gamma(2n) = \frac{1}{2}(2n-1)!$

$\frac{1}{2}\,0! = \frac{1}{2}$ $\quad n=\frac{1}{2}$

$\frac{1}{2}\cdot 1! = \frac{1}{2}$ $\quad n=1$

$\frac{1}{2}\cdot 3\cdot 2 = 3$ $\quad n=2$

$\frac{1}{2}\cdot 7\cdot 6\cdot 5\cdot 4\cdot 3\cdot 2$ $\quad n=4$ de Vauco valu

$= 42\cdot 20\cdot 3$

$= 840\cdot 3$

$= 2520$

The RHS is harder

and

Ciotti eq (8)

is ~~there~~ high accuracy interpolation formula

$$b(n) = 2n - \frac{1}{3} + \frac{4}{405}\frac{1}{n} + \frac{46}{25515}\frac{1}{n^2} + \frac{131}{1148175}\frac{1}{n^3} + \frac{2194697}{30690717750}\frac{1}{n^4} + O(n^{-5})$$

Better than all previous formula

To 4-term they get relerr $< 6\times10^{-7}$ for $n \in [1, 10]$

3034) $\Upsilon_{\odot}$ and Υ (Wik) Mass-to-light ratio

$\Upsilon_{\odot} = 5133 \frac{kg}{W}$ and $\Upsilon = \frac{L}{M} = \Upsilon_{\odot} \frac{M_{\odot}}{L_{\odot}}$

counting dark matter — Most galaxies $\Upsilon \approx 2-10$ but UFD $\Upsilon \approx 100-200$

5) a) Plot of $M_V = -\log I_V(R=0) + C$ in magnitudes versus M_V of whole galaxy

C-32

Fig 3.4

dex M_M

10^8 10

5×10^2

15

I_V (mag per arcsec²)

10^{10} 20

30

-24

10^{10} dex

$5 \times 2 = 10$

Quality

Narrow branches on CMDs

M

B-V

M/L high but low overall brightness

no star formation now

UCD, S Wik ellipticals stripped of gas in galaxy clusters

Ellipticals & bulges only

So Not in galaxy clusters mostly

MW Globular Clusters also metal poor & old. But star cluster from Dwarf galaxies: GCs differ

1) stars all born at one time (nearly)

2) No dark matter halo

3) No SMBH at all

4) more compact except UCDs

In a star formation region

Ancient from $t \approx 300$ Myr cosmic.

MW

disks only

M31 (And) LMC SMC

disk-like

BCDs Blue compact Dwarf star forming

formed from tidal streams

Very dark $[Fe/H] \approx -2.6$ rather dense & metal poor

Local Group dwarfs (see p. 170) (some stripped of HI gas, by passing near MW, M31, M33)

$10^2 - 10^5$ stars

very high M/L

Pegasus W $\frac{M}{L} = 200 \frac{M_{\odot}}{L_{\odot}}$

Most galaxies $M/L = 2$

-15

10^6 dex

UFD ultrafaint dwarf

M_V (Quantity) Absolute V-magnitude

only ~5% Baryonic: MW: mass

$10^{12} M_{\odot}$

No sharp lines.

Ci-29

define dwarfs $M < 10^{?} M$ $0.1 M_M$

$L < 0.1 L_{MW}$

$10^{11} L_{\odot}$

Wik say dwarfs in range $10^3 - 10^8$ stars

Mass-to-light ratio (Wik)

3034

b) Progression on Magnitude system

$$B = B_0 \, 100^{-M/5} = 10^{-\frac{2}{5}M} = 10^{-0.4M}$$
$$= b^{-M}$$

base = 2.511886432... hardly ever seen.

brightness or passband or something Flux (not luminosity)

not so far from natural base e = 2.718... not that it matters

So 5 magnitudes is change in brightness by a factor of 100. and in the wrong way.

The dead hand of the past condemns us to magnitude — Ptolemy (c.100 — 170 CE) classified stars as 1st to 6th mag: brightest to faintest to naked eye in his star catalog

N. R. Pogson 1829 — 1891 regularized it

We should just have replaced it by a right way scale dex $b = b_0 10^D$ and sometimes we do when really want to understand a plot → color-color plots are the worst

We can all agree

I am NOT going to get into distance modulus — oh what the heck

3034b

~~H~~ ~~however~~ ~~absolute~~
magnitude is ~~flux~~
magnitude at 10pc

$$F = F_{10}\left(\frac{R_{10}}{R}\right)^2$$ flow luminosity scales

$$10^{-.4m} = 10^{-.4M_A}\ 10^{-.4\mu}$$

$$\therefore m = M_A + \mu$$

distance modulus
Wik say μ
common
symb

$$\left(\frac{R_{10}}{R}\right)^2 = 10^{-.4\mu}$$

$$2\log(R_{10}/R) = -.4\mu = -\tfrac{2}{5}\mu$$

$$\mu = -5\log(R_{10}/R)$$

$$= 5\log(R/R_{10})$$

$$\mu = 5\log R - 5\log R_{10}$$

$$\mu = 5\log R - 5$$

in parsecs.

So at least μ grows with distance in right way
scale

What in R is in Mpc?

$R_p = R_{Mpc}\left(\frac{10^6 pc}{1 Mpc}\right)$

Expand μ Mpc and conversion factor
factor of unity

~~$R_{pc} = 10^{-6}R_{Mpc}$~~

~~$\mu = 5\log R_{Mpc}$~~

as usual for galaxies

$$\therefore \mu = 5\log R_{Mpc} + 30 - 5 = 5\log R_{Mpc} + 25$$

Conversion of bases (3034.

$$x = b_1^{y_1} \qquad x = b_2^{y_2}$$

two bases

logarithm of x for those bases

general base b

$$\log_b x = \log_b x$$

$$y_1 \log_b b_1 = y_2 \log_b b_2$$

$$y_2 = \left(\frac{\log_b b_1}{\log_b b_2}\right) y_1$$

usually b is one of b_1 or b_2

say b_2 is $= e$ natural base

b_1 is 10 common base

$$y_2 = \frac{\ln b_1}{\ln b_2} y_1 = \frac{\log b_1}{\log b_2} y_1$$

$$y_2 = \ln(10)\, y_1 = \frac{1}{\log e} y_1$$

$$y_2 = (2.302585\ldots) y_1 = \left(\frac{1}{0.43429448}\right) y_1$$

inverses of course

3 034d

6) 'R$_e$ VS M$_*$ C-33 Fig 3.5 | 3035

effective radius stellar mass

See p. 3036

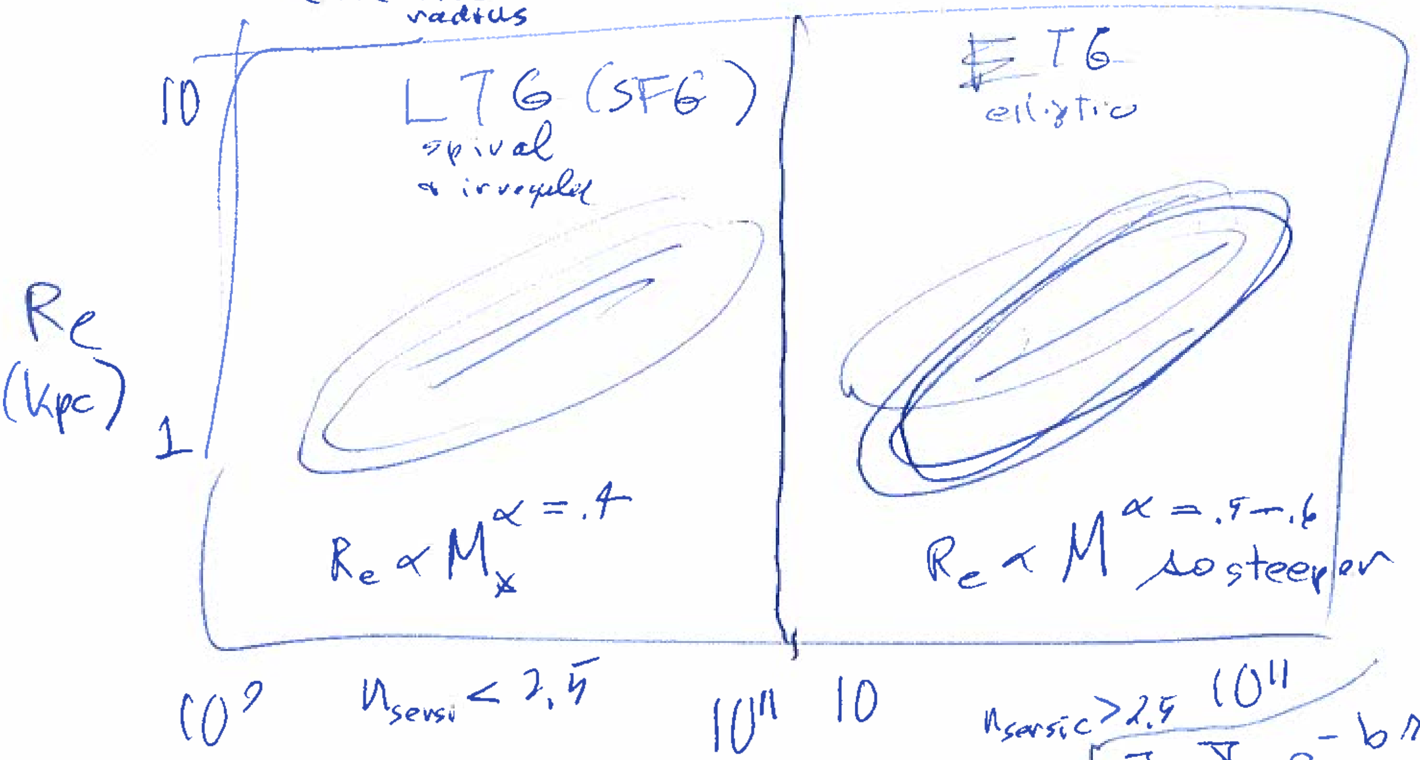

$I = I_{x_0} e^{-b x^{1/n}}$ C-31

$x = \frac{R}{R_e}$

as $n\uparrow$, more concentrated light at center

$M_*/M_\odot$

Not ~~total~~ mass

$M_* < 0.03\, M_{DM}$

Dekel 2019
p. 2
(Golden mass paper)

Theoretical understanding ~~IM sim~~ from simple analytic formulae is probably not possible.

The statistical properties of galaxies from large-scale structure (very big) formation calculations (e.g., Illustris, TNG, Eagle) must be compared to statistical properties of galaxies

3036

— ~~there~~ are many structure formation simulation but most are limited to certain aspects

only the big ones are ~~and~~ universal
— from primordial ingredients to cosmic present trying to get all features.

— The big ones overall do well but, of course, on many fine points less well.

And therefore constitute strong support for Λ-CDM and not for MOND

(MOND does do evolution so well is my understanding Ken N. told me that)

still a good approximation

If Λ-CDM needs revision or replacement due to tensions (~~and the~~ e.g., Hubble) the replacement will still be much like Λ-CDM overall

Plot Fig 3,5 C-33 L30 36a

Redux

Sersic idex

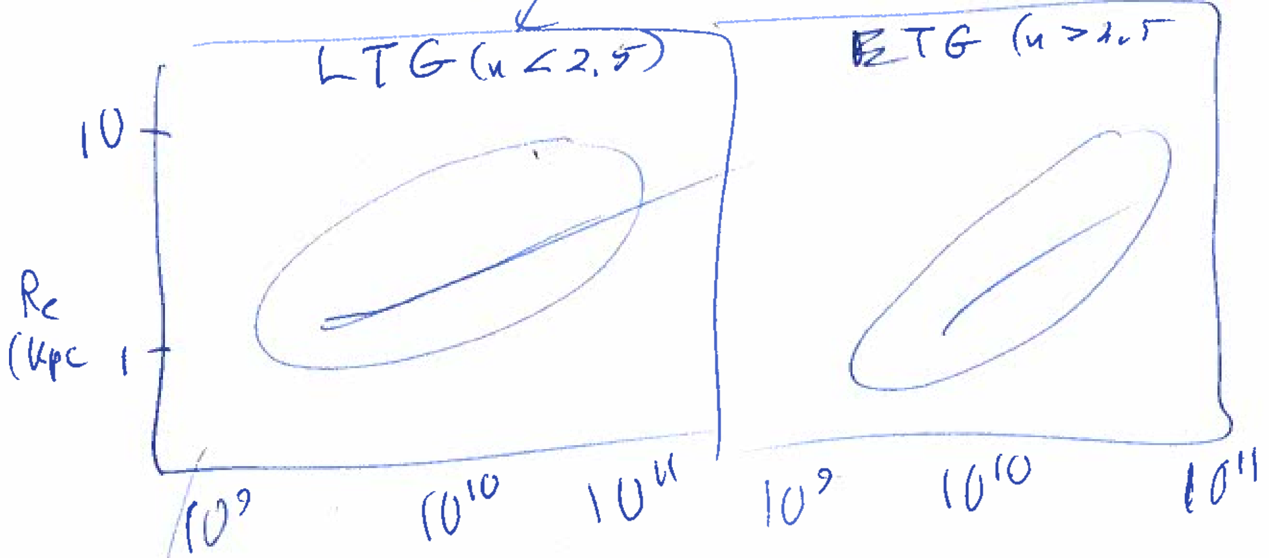

$\log (M_*/M_\odot)$

mass in stars

dark matter halo $M_{DM} \gtrsim 30 M_*$

Lots of scatter but

$$R_e \propto M_*^\alpha$$

$\alpha \simeq 0.4 = \frac{2}{5}$
and smaller for lower mass LTGs

$\alpha \simeq 0.5 \to 0.6 = \frac{1}{2}$
for ETG

A tiny bit of correlation.

Data to be fit
by (large scale) structure formation simulations.

3036b

7) Plot Fig. 3.6 C 34-36
SED of Galaxies

See p. 3036a

Note scaled to some overall mass to galaxies of each type can combined

a) Stars - mixture of blackbody spectra of many temperature since star photospheres approximate blackbodies.

$$B_\lambda = \frac{2hc^2}{\lambda^5}\frac{1}{e^x - 1} \qquad x = \frac{h\nu}{kT} = \frac{hc}{kT\lambda}$$

$$B_\nu = \frac{2h\nu^3}{c}\frac{1}{e^x - 1}$$

But superimposed absorption lines from cooler layers above photosphere

Driver et al. 2019

(30364)

$E^{1st}_{He} = 24.587...$ eV

$\lambda^{1st} = 6 \times 10^{-2}\ \mu = 60$ nm

$E^{2nd} = 54.4177...$

$\lambda^{2nd} = 2 \times 10^{-2}\ \mu m = 20$

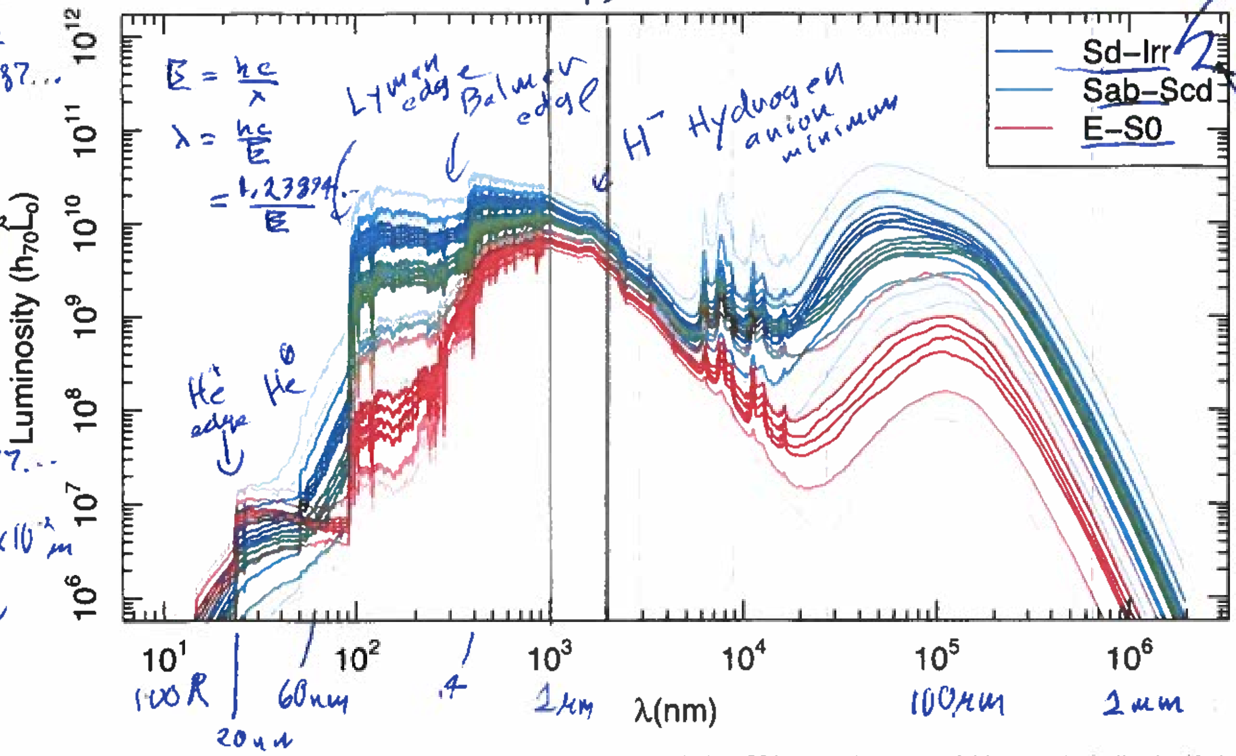

Star forming and so hot young blue stars; peak of black body spectrum shift to blue

Figure 23. The panel shows the 10, 25,45,50,55,75, and 90 percentiles for the full GAMA PDR SEDs for the $z < 0.06$ morphologically classified sample presented in Moffett et al. (2015). The data are initially scaled to the same mass and then at each wavelength point the quantiles derived which then collectively trace out the quantiles over wavelength. The spread at each wavelength therefore directly reflects the spread in the mass-to-light ratio at that wavelength.

(as expected), indicating that this region is optimal for single band stellar mass estimates. However, the constant gradient in this region implies that near-IR colours provide little further leverage to improve the stellar mass estimation beyond single band measurements. Conversely the smooth variation of SED gradients in the optical from low to high stellar mass ratios, imply that optimal stellar mass estimation may arise from the combination of a single band near-IR measurement combined with an optical colour (see also discussion in Taylor et al. 2011). Fig. 23 highlights the known strong correlations between UV flux, far-IR emission and stellar mass-to-light ratio with all being amplified or suppressed in Sd/Irrs or E/S0s, respectively. However, that all galaxies seem to contain some far-IR emission may be a manifestation of the MAGPHYS code tending to maximize dust content within the bounds as allowed by the far-IR errors. Curiously the Sabc (green) provide a very narrow range of parameters, perhaps indicating a close coupling between star formation, dust production, and the mass-to-light ratio – arguably indicative of well-balanced self-regulated disc formation/evolution. The greater spreads in the early (red) and later (blue) types are perhaps indicative of the progression through various stages of quenching (ramping down) and unstable disc formation (overshoot), respectively. In particular, Agius et al. (2015) found an unexpectedly high levels of dust in a significant (29 per cent) population of the GAMA-E/S0 galaxies consistent with a range of E-So SEDs. Note also the results presented on observed correlations between the star formation rate, specific star formation rate in da Cunha et al. (2010) and Smith et al. (2012), see also interpretation in Hjorth, Gall & Michalowski (2014). A detailed exploration of these phenomena are beyond the scope of this paper but the potential is clear particularly in conjunction with the existing group (Robotham et al. 2011) and large-scale structure (Alpaslan et al. 2014) catalogues.

4.1.1 Inspection of individual objects

We explore individual SEDs for one hundred systems randomly selected (IDs 47500-47609). Approximately 5–10 per cent are found to have one or more significant outlier(s) in the photometry but otherwise good MAGPHYS fits are found for all 100 systems. In approximately 50 per cent of cases the far-IR photometry is essentially missing (due to the shallowness of the far-IR data), hence flux and/or redshift cuts are advisable depending on the science investigation to be conducted. Fig. 24 shows four example galaxies which include a nearby bright system (G47152, $z = 0.082$), a nearby faint system (G47157, $z = 0.074$), a higher redshift crowded system (G47609, $z = 0.282$), and a known far-IR lens system (G622892, $z = 0.300$; Negrello et al. 2010, recently shown to exhibit a spectacular Einstein ring, the very high far-IR flux is evident). The panels on the left show the combined *giH* colour image from a combination of VIKING and SDSS data. Overlaid (green dotted lines) are apertures for the main object and nearby systems in our bright catalogue. The right-hand panels show the 21-band measured photometry (green data and error bars) in units of total energy output (λL_λ in units of h_{70} W) at the filter pivot-wavelength divided by $(1 + z)$ (i.e. rest wavelength). The red and blue lines show the attenuated and unattenuated SEDs from the preliminary MAGPHYS fits. Purple circles show the flux from the attenuated SED curve integrated within the filter bandpasses given in Fig. 1. The lower portion of the panel shows the residuals expressed as the ratio of the observed flux to the measured flux. Included in the error budget is a 10 per cent flux component added in quadrature to mitigate small systematic zero-point offsets at facility boundaries. Comparable plots for all 221k systems with redshifts are provided via the GAMA Ψ online cutout tool (http://gama-psi.icrar.org/).

3036d

Original

L 3039

H lines
H Balmer lines in visible

Then ionization edges
shown in the

– cooler stars ~~$M_* \leq M_\odot$~~
$M \lesssim M_\odot$

have strong H^- hydrogen anion
absorption

so it
has no
lines.

$$E^{ion} = 0.754195(19)\,eV$$
(Wik)

Hans Bethe proved it must
exist theoretically
in 1929

– no bound excited states
proven in 1977

Always ~~a minority~~
a minute species
and requires
low ionization
metal electrons.

But very strong
bf ~~ff~~ ff opacity and so importance all out
of proportion to abundance

↑
higher energy required
(lower λ)

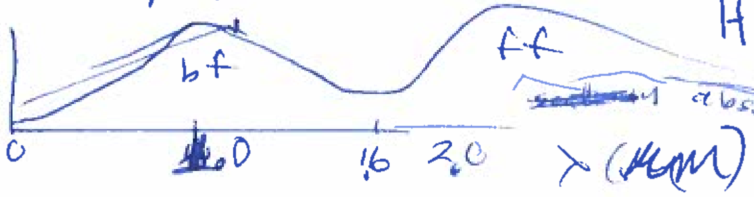

HM-206
-208

~~[illegible]~~ absorption-emission
equality
LTE

3038

b) Dust extinction

In LGTs (spirals Irr) also extinction & very little in EGs (ellipticals)

dust dependent parameter $R_V = 3.1$ fiducial value (C-81)

$A_V = R_V E(B-V)$

$E(B-V) = (B-V) - (B-V)_0$
observed

$\frac{A(\lambda)}{A(V)}$

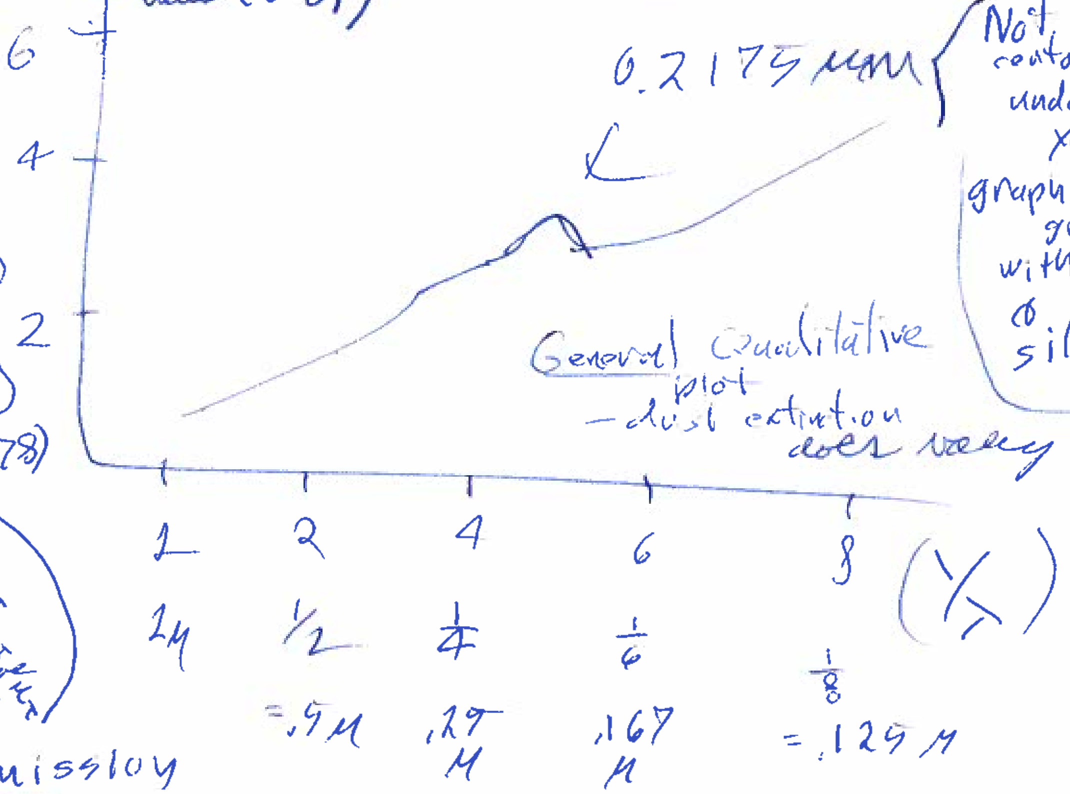

Not certainly understood yet. graphite grains with PAHs & silicate

– dust extinction does vary

$A_\lambda = -2.5 \log\left(\frac{F_\lambda}{F_{\lambda 0}}\right)$

$F_\lambda = F_{\lambda 0} e^{-\tau_\lambda}$ (C-78)

$A_\lambda = -2.5 \log e^{-\tau_\lambda}$

$= +2.5 (\log e) \tau_\lambda$

$\simeq \tau_\lambda$ ← A_λ came from τ_λ

c) Dust emission

The dust absorbs UVOIR and emits as grey body emission in farther IR (C-522, 36)

$Q_\lambda B_\lambda$, $Q \propto \lambda^{-\beta}$

Not same as grey opacity HH-569 -588

β { 1 amorphous
2 metallic

Some feature of surface of grain that absorbs some energy and re-emits in other bands somehow

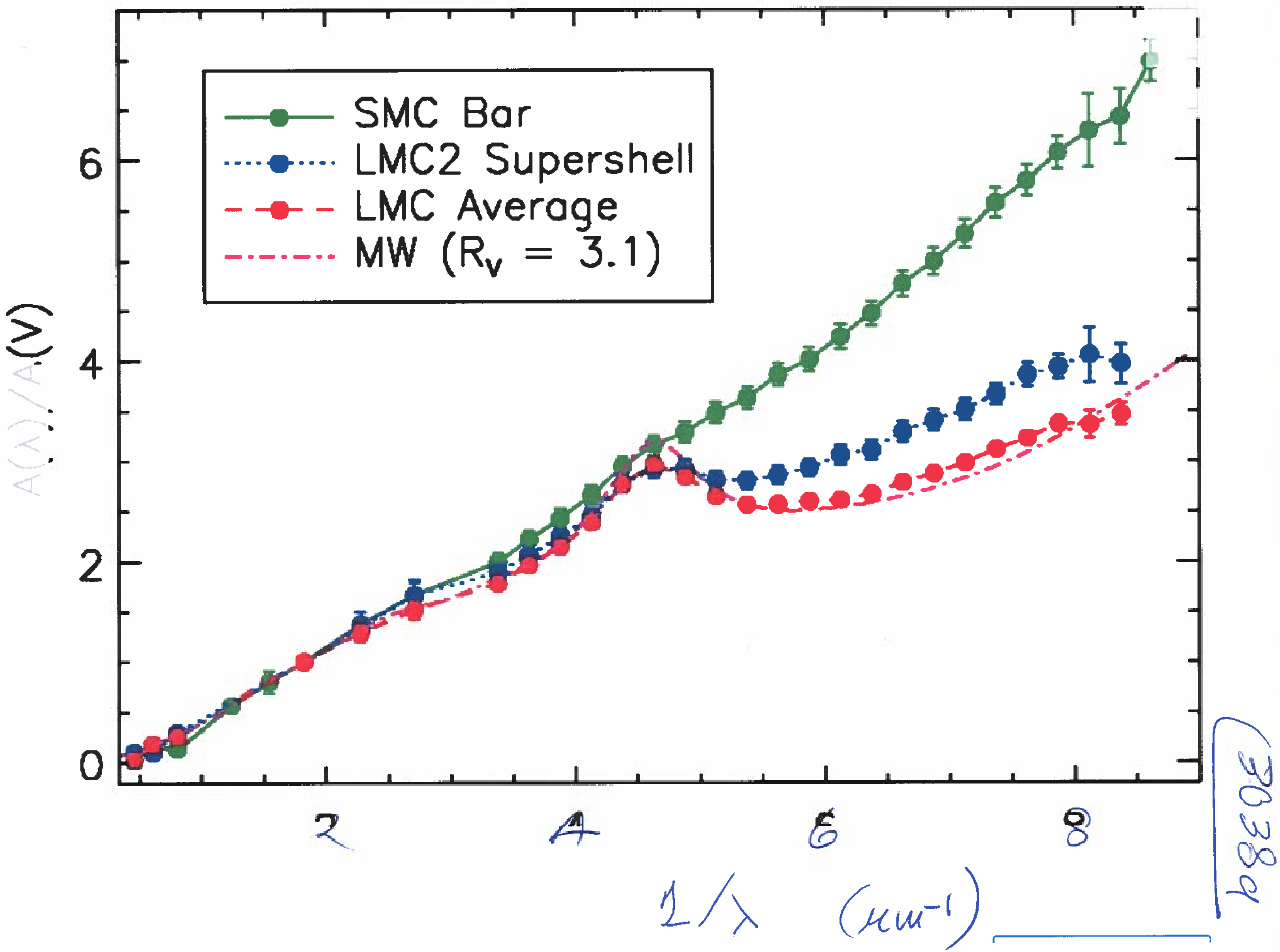
SMC Bar
LMC2 Supershell
LMC Average
MW (R_V = 3.1)
6
4
2
0
A(λ)/A(V)
2
4
6
8
1/λ (μm⁻¹)
3038a

Plot showing the average extinction curves for the MW, LMC2, LMC, and SMC Bar.[29] The curves are plotted versus 1/wavelength to emphasize the UV.

Karl D. Gordon - Own work

File: Interstellar extinction ave curves local group.png

Created: 1 January 2003

Average UV-NIR extinction curves for MW, LMC, and SMC (or regions therein). From data published in Gordon, K. D. et al. (2003, ApJ, 594, 279).

About Media Viewer

30386

3039

4) Note ~~the~~ ~~[illegible]~~ LTGs do have some dust emission, but the plot scale is logarithmic axis so of order $\frac{1}{10}$ of EGTs

— To first order we say ~~that~~ LTGs have no dust

What happens to it from the pre-elliptical phase (pre merger often)

— over gigayears it erodes away — UV
— x-ray
— hot gas

Space weathering

(?

— Not replenished much
— no SNe and ~~[illegible]~~ dust production from post-main sequence stars.

LTGs have gas — but mostly hot

Somehow bue Largeon the inflow + outflow to SMBH heats most gas and convert bubbles plume from inner region

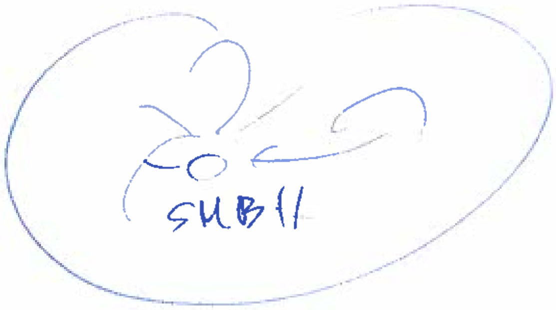

3040 emits in X-ray but weakly → now seen.

There is some cold gas and CO emission is observed for them

e) Diffuse emission from gas

$H\,II = H^+$ region

UV – ionization followed by recombination cascades

– in visible the Balmer lines

$H\alpha$ 0.65628 nm
$H\beta$ 0.486132 nm
$H\gamma$ 0.434046 nm
$H\delta$ 0.410173 nm

mix altogether create pink or magenta "true" in color images

Also all kinds of emission lines from Molecular clouds

molecules of all kinds H_2

molecular Hydrogen of course most key one but is almost invisible

dust shields molecules from UV and that prevents dissociation.

– the molecules

strongly emit cooling the gas, which loses pressure support which can then collapse to form new stars.

By the way star formation has low efficiency ~ 2-3 % (e.g. Krruijssen et al 20.. arXiv 905.0..) of molecular gas goes into new stars before star formation broken

The hot young blue stars tend to evaporate dust and disperse it via SNe they ignite the cloud that fed them

Also forbidden and semi-forbidden line emission

forbidden lines are forbidden by ~~the~~ main process (dipole emission) but happen by others.

happen in low density environments.

— recombination cascades populate their upper levels (metastable levels)

→ Low collisions rates prevent collisional de-excitation

3042

→ seen from planetary nebula

→ in nebular supernovae

Iron peak elements
- iron
- cobalt
- nickel have a lot of metastable lines and so lots of forbidden lines

[Ca II] and [O I]   C II]

square brackets mean forbidden

semi forbidden

both have well known ~~famous~~ forbidden lines

See Ca II grotrian diagram

Funny ~~Units~~ on Vertical Axis of Plot
- 36 don't explain it!
- original paper is brief and unclear

Think I've figured it out.

f) 21-cm line See p. 3034c-d

— a strongly forbidden line

3042c

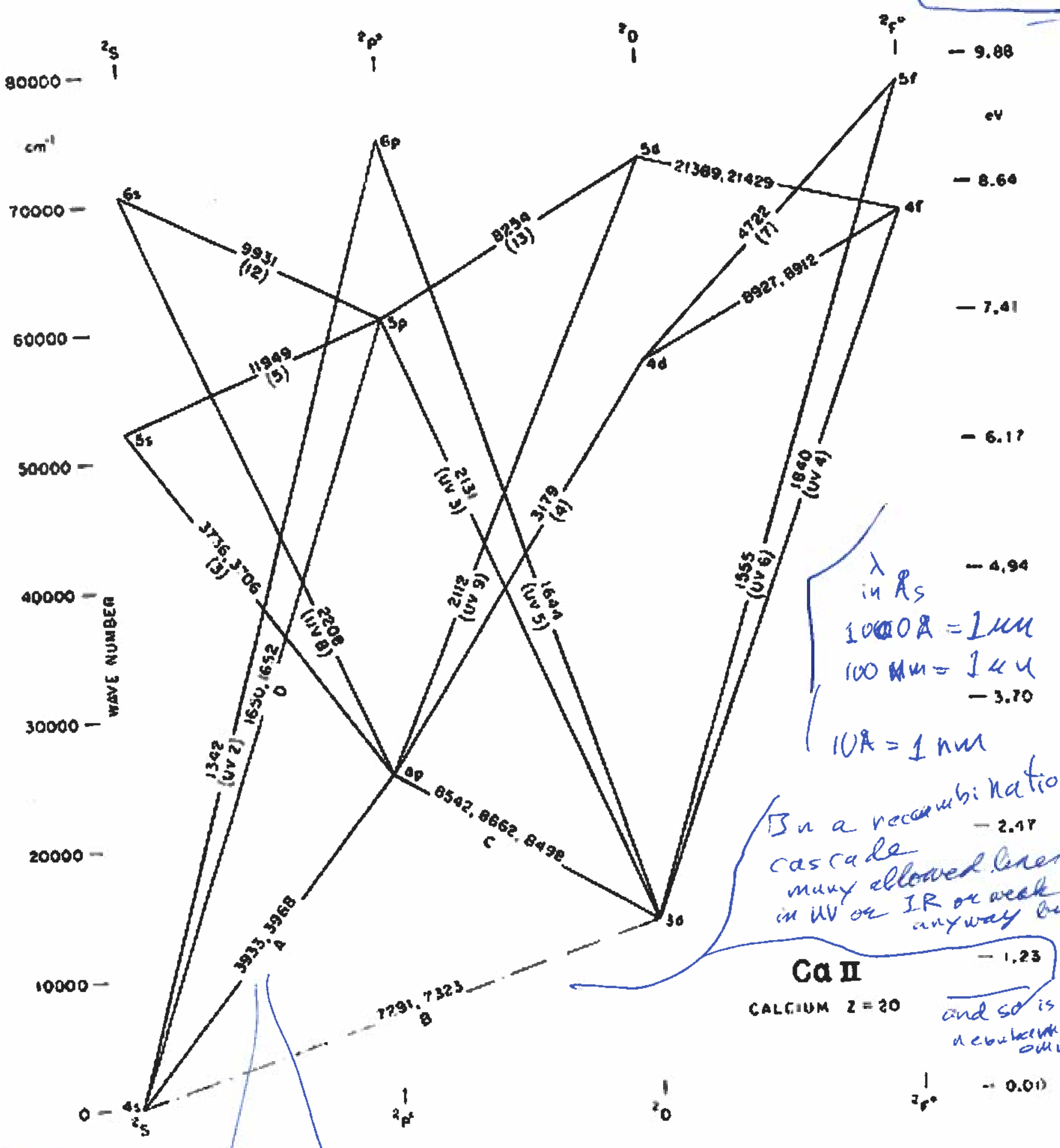

λ in Ås
10000 Å = 1 μm
100 nm = 1 μ
10 Å = 1 nm

In a recombination cascade many allowed lines in UV or IR or weak anyway but 7330 doublet and so is strong nebular emission

Non-thermal fast electrons from $Co^{56} \to Fe^{56}$ decay create γ-rays then an ionization cascade of fast electrons that ionize

Ca II H&K lines very strong since ~~from the ground state~~ where e most of the time.

Moore & Merril 1968

In nebular SNe, the H&K lines still seen in absorption for a long time after other lines are in nebular emission from recombination.

30426

Original

3042

Image 1 Caption: An **ABSTRACT** diagram of the ground state hyperfine levels of atomic hydrogen (H I): i.e., the parallel spin higher energy hyperfine level (F=1 state) and the antiparallel spin lower energy hyperfine level (F=0 state which is the true absolute ground state).

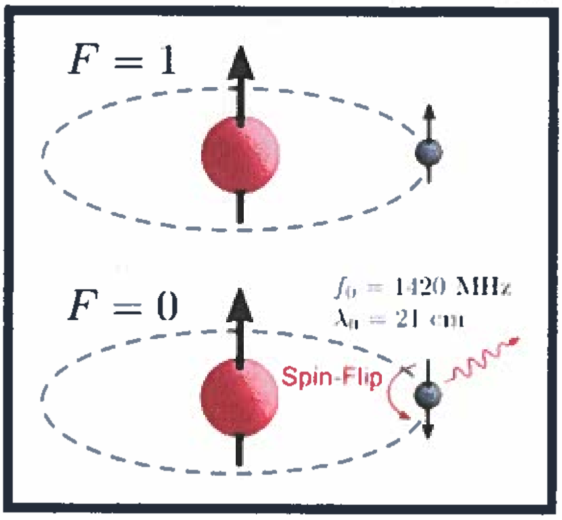

The atomic transition from the F=1 state to the F=0 state emits the hydrogen 21-centimeter line (21.1061140542 cm, 1420.4057 5176 67(9) MHz ≅ 1420 MHz). This transition line is in the radio band (fiducial range 3 Hz -- 300 GHz = 0.3 THz, 0.1 cm -- 10**5 km).

Features:

1. As aforenoted, the diagram is **ABSTRACT**. Both proton (the hydrogen nucleus colored in red) and the electron (colored in grey) exist in a spherical cloud-like superposition of positions: the proton in small cloud at the center of the large electron cloud.

2. Now most elementary particles have spin, an intrinsic and invariable angular momentum. In fact, the only known spin 0 elementary particle (i.e., elementary scalar boson) is the Higgs particle (Wikipedia: Scalar boson: Scalar).

3. The proton and electron both have spin 1/2 (in units of the Planck constant divided by 2π: symbol $\hbar$).

   >2< 1

   Quantum mechanics dictates that only two alignments are possible for the proton and electron: the parallel F=1 state and the antiparallel F=0 state.

4. The downward spin-flip transition from F=1 state to F=0 state emits the emission spectral line the hydrogen 21-centimeter line (21.1061140542 cm, 1420.4057 5176 67(9) MHz ≅ 1420 MHz).

   In space, the downward spin-flip transition is almost always a spontaneous emission (only very rarely a stimulated emission). The putting of the hydrogen atom in the F=1 state may be due to a collisional excitation (and therefore controlled by the local temperature and density of the gas in space) or to the spontaneous emission from a higher energy level that was excited by a photon absorption, a collisional excitation, or following a recombination following at photoionization.

5. The mean lifetime of the F=1 state for the hydrogen 21-centimeter line is 10.9 Myr (see Wikipedia: Hydrogen line: Cause). The mean lifetime is so huge because the atomic transition is a highly forbidden transition. "Forbidden" in this context means forbidden by the most usual atomic transition mechanism, but allowed by weaker atomic transition mechanisms.

6. Because mean lifetime of hydrogen 21-centimeter line is so huge, it probably can **NEVER** be measured in the laboratory. You simply need too huge a sample of low density cold neutral atomic hydrogen gas for the spontaneous emission of the hydrogen 21-centimeter line to be observed. The mean lifetime has to be calculated theoretically from quantum mechanics. Note stimulated emission of the hydrogen 21-centimeter line can be seen in the laboratory using a hydrogen maser (see Wikipedia: Hydrogen line: Cause).

7) But though it probably can **NEVER** be measured in the laboratory, the vast volumes of low density cold neutral atomic hydrogen gas in space allow easy detection of the spontaneous emission of the hydrogen 21-centimeter line from that realm. The observation hydrogen 21-centimeter line from space is one of the key tools of radio astronomy (see Wikipedia: Hydrogen line: Uses).

7. Image 2 Caption: A Grotrian diagram of the fine structure and hyperfine structure of atomic hydrogen (H I). The angular momentum coupling of the different angular momenta causes energy level splitting. The Grotrian diagram is **NOT** to-scale.

Recall a Grotrian diagram is a diagram illustrating the energy levels of an atom or molecule, either of which could be an ion.

The 2 lowest energy levels are those shown in Image 1.

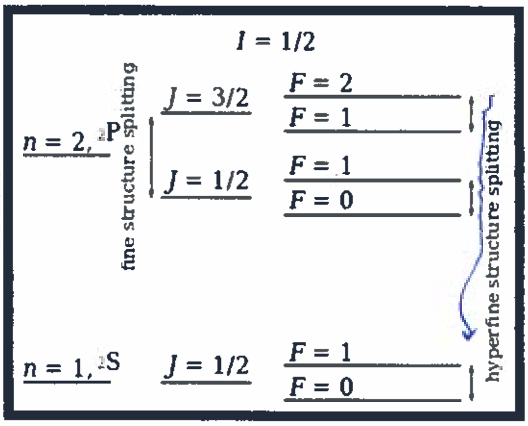

Images:
1. Credit/Permission: User:Tiltec, 2009 Public domain.
Image link: Wikimedia Commons: File:Hydrogen-SpinFlip.svg.
2. Credit/Permission: User:DJIndica, User:Edudobay, 2010 Public domain.
Image link: Wikimedia Commons: File:Fine hyperfine levels.svg

Local file: local link: atom_001_h_001_21_cm_line.html.
File: Atomic file: atom_001_h_001_21_cm_line.html.

9) Scaling of Fig. 3.6 (Ci-35) | B043

Fig 3.6 has a funny mass scaling ~~of~~ ~~pt~~ galaxies of the same type but different masses so that they can be compared in SED properties. Ci-35 don't explain the scaling. The original paper is buried to obscurity (Driver et al 2016). So I can only guess at what the scaling is (Maybe wrongly)

First $v_{\text{recession}} = H_0 r$ but $v_{\text{rec}} = v_{\text{redshift}}$ for nearby universe.

So $r = \dfrac{v_{\text{red}}}{H_0} = \dfrac{v_{\text{red}}}{70}\dfrac{70}{H_0} = r_{70}\dfrac{1}{h_{70}}$ where $h_{70} = H_0/(70\ \frac{\text{km/s}}{\text{Mpc}})$ since 70 is our fiducial value currently. It can only be ~5% wrong (we think).

Now for galaxy i

$$F_{i\lambda} = \frac{L_{\lambda i}}{4\pi r_i^2}$$

$$F_{i\lambda} = \frac{L_{\lambda i s}}{4\pi r_{i70}^2 h_{70}^{-2}}\left(\frac{M_i}{M_s}\right)$$ where M_s is some scale mass galaxies of type S.

Now $M_i \propto \rho_{\text{average}} R_i^3 = \rho_{\text{ave}}(\theta_i r_i)^3 = \rho_{\text{av}}(\theta_i r_{i70})^3 h_{70}^{-3}$

ρ_{average} for galaxy of type S

R_i is characteristic size of galaxy i

$$\therefore M_i = M_{i70} h_{70}^{-3}$$

$$L_{\lambda i s} = F_{i\lambda} 4\pi r_{i70}^2 h_{70}^{-2}\left(\frac{M_s}{M_{i70}}\right) h_{70}^3 = \frac{F_{i\lambda}4\pi r_{i70}^2\left(\frac{M_s}{M_{i70}}\right)}{L_\odot}(L_\odot h_{7\ldots}$$

all determinable from data except M_s may be assumed.

is ... un...

3044) 8) Luminosity Function (LM)
Schechter (Luminosity) Function

$\Phi(L)\,dL$ is the number of galaxies in dL per volume
conventionally Mpc^{-3}

Paul Schechter (1976)
(1948 May 30 —
whom I used to see a CfA in 1991–1993 when he came over from MIT)
came up with a fitting function.
— an original version the Press-Schechter function had a theoretical argument,
but Schechter noticed ~~or gave~~ an empirical generalization worked well. As with the Sersic Profile for surface brightness
probably competing effects give rise to parameters,
and the only "derivation"
is showing a full ΛCDM (or replacement model)
with a full simulation from cosmic dark ages the now derived it — though for each distinct parameter value there may be a analytic derivation,

$$\Phi(L)\,dL = \Phi^*\left(\frac{L}{L^*}\right)^{\alpha} e^{-\left(\frac{L}{L^*}\right)}\, d\left(\frac{L}{L^*}\right)$$

3045

Φ^* , α , L^* are parameters

overall scale

power law

division parameter between power and exponential

If $\alpha > 0$

$$f(x) = x^{\alpha} e^{-x}$$

$$\frac{df}{dx} = \alpha x^{\alpha-1} e^{-x} - x^{\alpha} e^{-x} = 0$$

$f(x_{max}) = \alpha e^{-\alpha}$

$$x_{max} = \alpha$$

Also integrable to finite value

$$\int_0^{\infty} x^{\alpha} e^{-x}\, dx = \cancel{x}!$$

$\alpha(\alpha-1)(\alpha-2)\ldots 1$ if α is integer

$\alpha(\alpha-1)(\alpha-2)\ldots \frac{1}{2}\sqrt{\pi}$ if α is half integer

α otherwise numerical integration

α the factorial function Anf-543

$\alpha = 0$ pure exponential
No observed case

But $\alpha < 0$

Diverges as $x \to 0$
and ~~not~~ ~~integrable to $x=0$~~
must use an x cutoff

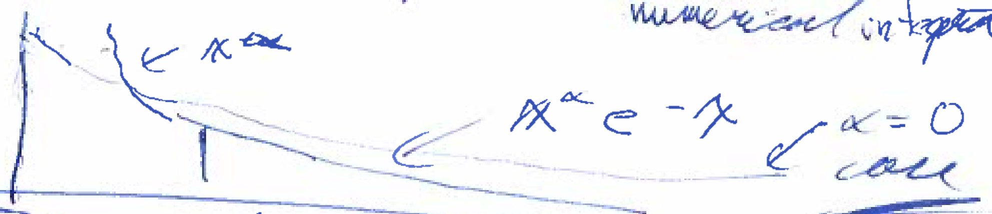

$x = 1$ is the transition

3906

$$\begin{rapolyfill}\end{rapolyfill}$$

$x = 1$

$L = L^*$

is called knee

$L < L^*$ low luminosity

$L > L^*$ high luminosity

In general

$$n = \int_{L_0}^{\infty} \Phi(L)\,dL = \Phi^* \int_{x_0}^{\infty} x^{\alpha} e^{-x}\,dx$$

$$= \Phi^* \gamma\left(\alpha+1,\ x_0 = \frac{L}{L_0}\right)$$

$$\Phi^* \Gamma(\alpha+1) \text{ for } x_0 \to 0$$

$= \Phi^* \alpha!$

In any case, integrating to $x = 0$ is probably pushing the fit too far even for $\alpha > 0$

$\alpha + 1 = z$ ← Not Redshift

$z = \alpha - 1$

converges to ~~+ve~~ value for

$z \leq -1$ diverges

See AJ-543 but to ~~+ve~~ value ~~for~~

$z \neq$ ~~-1~~, ~~-2~~, ~~-3~~, ~~-4~~, (-5, -6), etc.

$\alpha \neq 0, -1, 2, \ldots$

[The formal $z!$ is defined differently for $z \leq -1$ see AJ-543]

3407

The Schechter function can also be written magnitudes, but who cares? I guess we have to put up with it
(~~dex will do for~~ dex would be better)

~~Finding the~~

Comparing Φ^*, α, L^*
as functions of redshift z
to large simulation (e.g., Illustris, TNG, Eagle)
is a test of ~~these~~ simulation
→ overall they do not badly
I understand
But lots of fine discrepancies
(I believe)

One would have to a up-to-date expert to be sure

Double Schechter function

$$\Phi(L)dL = \cancel{[\Phi_1^*(x) + \Phi_2^*]}$$

$$= [\underbrace{\Phi_1^* x^{\alpha_1}}_{\text{spheroidal}} + \underbrace{\Phi_2 x^{\alpha_2}}_{\text{disk}}] e^{-x} dx$$

galaxies of one type can be fit with a single Schechter together
but ETGs & SFGs ~~are better~~ are better fit by double Schech

3048

Knee magnitude → line between low & bright galaxie

single Schechter

Galaxies, $z \in [.025, .06]$	M^*_r r-band	Φ^* (10^{-3} Mag^{-1} Mpc^{-3})	α	$\rho_{L,tot}$ ($10^7 L_\odot$ Mpc^{-3})
all types	-21.17	4.00	-1.12	16.02
E	-21.67	1.22	-0.64	3.88
S0-Sa	-20.25	2.16	1.08	4.50
SB0-SBa	—			
Scb-Scd	-19.83	3.90	0.64	3.81
SBab SBcd				1.91
Sd-Irr	-18.46	11.56	-0.40	

SDSS $g = 0.4886$ which really blue light

0.6165 μm mean wavelength

Recall these are parameters of all type not same for the type

must have a cutoff for divergent Φ's

12.19

4.00

There Add but must unlisted types that contribute

a) But bolometric is harder to get accurate, Blue bands more affected by dust extinction

) Blue bands biased it more to hot young blue stars which contribute ~~[illegible]~~ more

~~but they~~ so due mass-to-light would be in blue bands

But what do R magnitudes mean — give bolometric or a color so we can tell it Blue or Red

We'd have to go back to the original paper to see why

Color B−V the smaller the bluer and hotter and more star forming ~~[illegible]~~

So b may contribute parameters in Φ(L)

In a blue band maybe not ~~[illegible]~~ red stars may be sig

The redder the colder, older, more quenched

r band better judge of overall likeness — b band of unlikeness

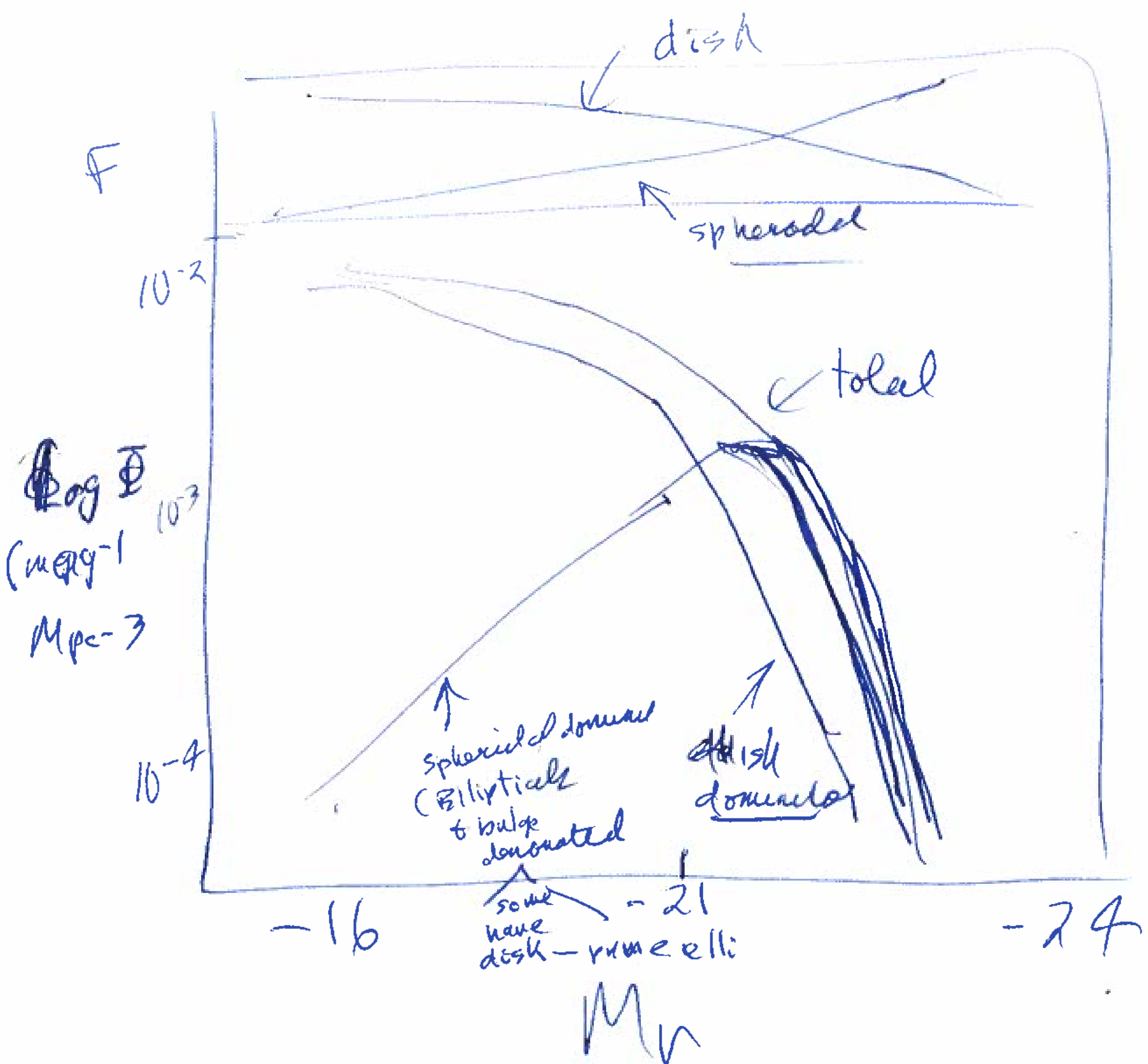

Relation
Log Luminosity
in r

⊙

$100 + 10^{\frac{2}{5}\cdot 3}$

$\simeq 10^3$

So disks dominated for M_r dimmer ~ −21

Spheroidal for M_r brighter ~ −21

Maybe incomplete for dwarf ellipticals.

Also disk dominated have star formation & so hot blue bright stars

7050

~~Mass~~ Stellar Mass function (SMF) | so Not including dark matter

2) & Schechter (Mass) function

It should be no surprise ~~that~~ luminosity & stellar mass should be correlated

A well known parameter of galaxies is the Mass to light ratio (Wik)

$$\Upsilon_{\odot} = 5133 \text{ kg/W}$$

Usually ~~other sources use~~ $\Upsilon_{\odot}$ is used as the unit (the Sun is the measure of all stars)

So
$$\Upsilon = \frac{y M_{\odot}}{x L_{\odot}} = \frac{y}{x}\left(\frac{M_{\odot}}{L_{\odot}}\right)$$

But this is total mass not stellar mass M_*

$$\Upsilon = \frac{y(M_{\odot})}{L(L_{\odot})}$$ and the units unit work out correctly

Typically galaxies have $\Upsilon = 2$ to 10 | Counts dark matter

Very dark matter dominated. but UFD = ultra-faint dwarfs have $\Upsilon \simeq 100 - 200$ or so

3051

Since Υ is of order a few there is only a modulation of Luminosity/mass function

Stellar mass only in Υ: $\Upsilon_* = \frac{M_*}{L} \approx 0.1$ very roughly

$$\Phi(M)\,dM = \Phi^* x^\alpha e^{-x}\,dx$$

$$x = \frac{M}{M^*}$$

M_* is stellar mass but M^* is the knee M_*

overall galaxy types a single Schechter

$M^*_\odot \sim 10^{11}$

which $\sim 0.1\, M_{\text{golden}} \sim 10^{12} M_\odot$ but all matter baryonic + dark

The mass above which most galaxies are quenched in modern universe but not the Milky Way yet $M \lesssim 10^{12} M_\odot$

The fiducial dried $M < M_*$ small $M > M_*$ large

and $\alpha = -1.3$

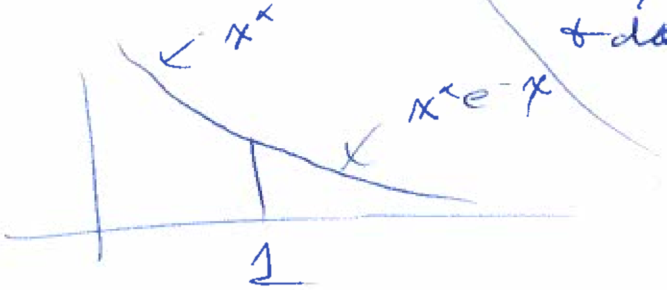

But a double schechter function works much better

$$\Phi(M)\,dM = \left[\Phi_1^* x^{\alpha_1} + \Phi_2^* x^{\alpha_2}\right] e^{-x}\,dx$$

$M^* = 10^{10.6} M_\odot$

for spheroid dominated $\alpha_1 = -0.43$

$\Phi_1^* = 4.18$

in units of $10^{-3}\,\text{dex}^{-1}\,\text{Mpc}^{-1}$

dex for mass Not magnitudes

disk dominated

$\Phi_2^* = 0.74$

$\alpha_2 = -1.5$

3052

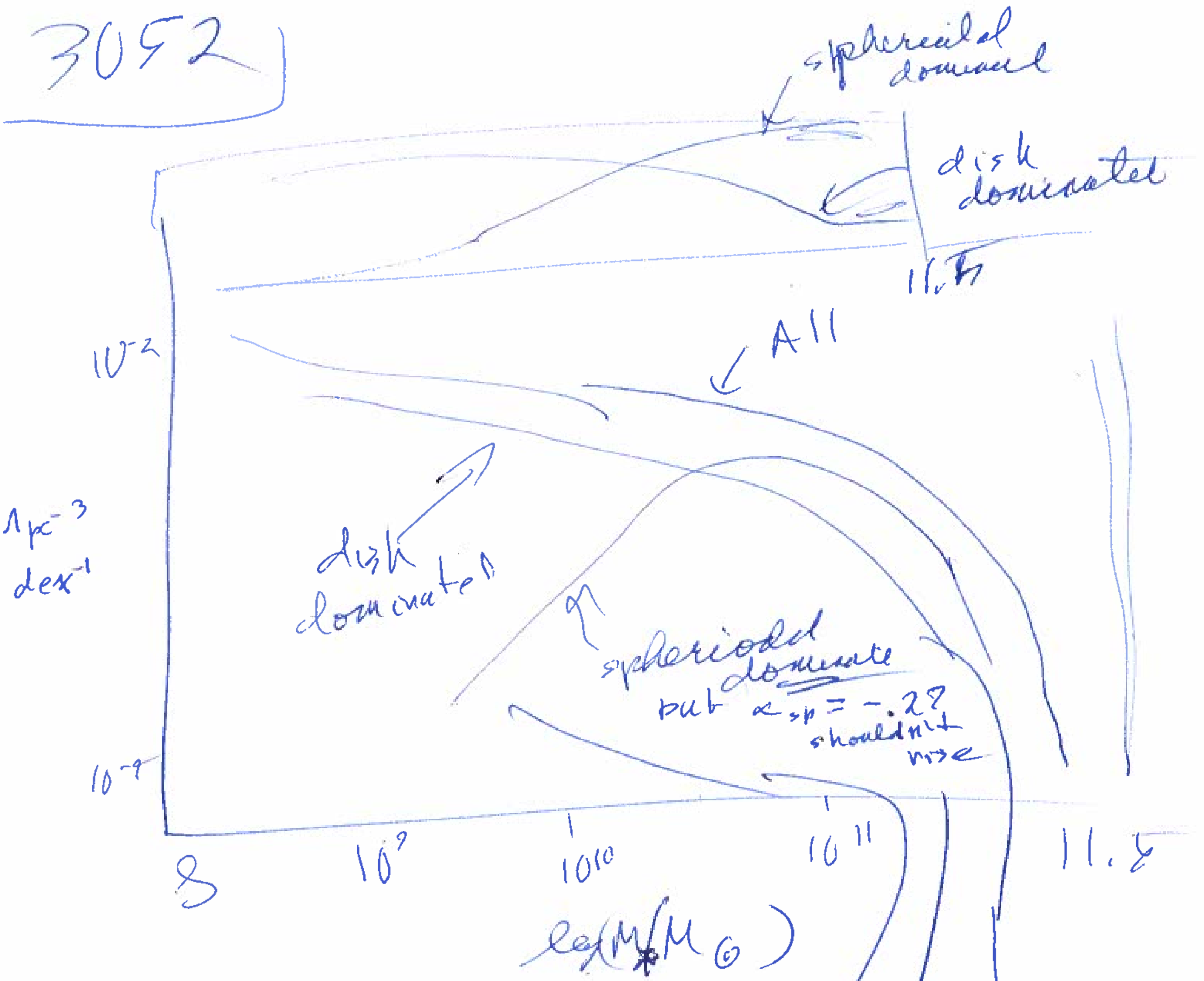

Same problem on C-46-47
and Kelvin 2014
p. 8 Fig
p. 12 Table